MEASUREMENT OF PARTICULATE MATTER IN SMOKE PLUMES FROM WILDLAND FIRES USING LIDAR TECHNIQUES

MEASUREMENT OF PARTICULATE MATTER IN SMOKE PLUMES FROM WILDLAND FIRES USING LIDAR TECHNIQUES.

Final Report
to Agreement 01-JV-112222049-254

Investigators

William Eichinger, Urska Koren
IIHR Hydroscience and Engineering
University of Iowa

Ronald A. Susott, Vladimir A. Kovalev
Fire Sciences Laboratory
Rocky Mountain Research Station
USDA Forest Service

I. OBJECTIVES

Wildfires and prescribed fires produce large quantities of smoke aerosols that can severely affect air quality and visibility. This, in turn, can result in health problems, car accidents, and airport and road closures. The purpose of this project is to assess the use of a portable scanning LIDAR to measure particulate matter levels in wildland fire smoke. This information will help managers and public officials predict and assess effects of wildland burning on air quality for better preparation for these events. The U.S. Forest Service is interested in investigating methods for determining particulate levels within smoke plumes from wildland fires. To accomplish this, a method must be developed to measure the particulate levels rapidly over a large volume. Currently no method other, than aircraft sampling, exists to rapidly determine particulate levels in large smoke plumes. Also involved are the need for improved lidar scanning methods, data inversion methods and data display. The goal of the Forest Service is a better understanding of aerosol movement in the atmosphere and improved smoke dispersion models.

Associated with this purpose, the following specific tasks were assigned.

- Identify scanning routines that may be used to measure particulate plumes from a forest fire. If a desired routine is not part of the existing lidar scanning capabilities, they will be programmed and the appropriate changes to the lidar data collection programs made.

- Conduct a field campaign to collect elastic lidar data during a forest fire. The data will be collected at locations and using scanning patterns and strategies designated by the Forest Service. The data will be taken at two wavelengths (0.532 and 1.064 microns), one at a time.

- Analyze and display the data in a manner consistent with the objectives of the experiment and the type of data collected.

- Identify methods for data analysis that take advantage of opportunities during the field campaign and the desire of the Forest Service to measure particulate matter concentration. It is anticipated that modifications of the current analysis routines will be required to accomplish this.

II. APPROACH

A. Lidar Technique. Lidar stands for LIght Detection and Ranging. The lidar systems are laser based systems that operate on principles similar to radar (RAdio Detection And Ranging) or sonar (SOund Detection And Ranging). In the case of lidar, a laser beam is used to scan the atmosphere over a desired range of directions and elevations. Light from the beam is scattered from molecules and particulates in the atmosphere. A portion of the light that is scattered back towards the lidar system is collected by a telescope and is measured with a photo-detector. Depending on the wavelength of the laser used and the optical processing done at the back of the telescope, many different types of information can be collected on the concentrations of various atmospheric constituents as a function of distance from the source.

The signal is digitized and analyzed by a computer to create a detailed image of the concentrations within the scanned region. Figure 1 is a schematic representation of the major components of a lidar system.

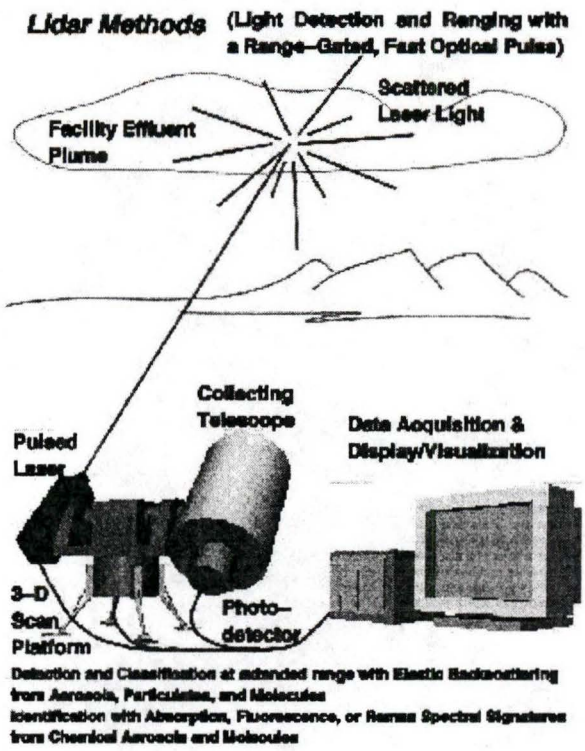

Figure 1: A block diagram showing the basic lidar concept and major components.

The advantage of the lidar technique for atmospheric work is that the spatial extent of the laser pulse is small (a few centimeters in diameter and about two meters long). This means that concentrations can be mapped to several kilometers with high spatial resolution (on the order of 1 to 3 meters). The advent of rapidly pulsed lasers, as well as the computers and electronics to take advantage of this, lead to the capability for high temporal resolution as well (as low as 20 seconds between horizontal or vertical scans). Thus one can map out the spatial concentration of particulates as a function of time and space, and watch processes as they develop.

B. Miniature Elastic Lidar. The lidar at the University of Iowa is contained in three carrying cases and a portable PC (figure 2). The first case contains the laser power supply and chiller. The second case contains the bulk of the lidar including the scanner motor power supplies and controllers as well as the power supply for the detector. The third case is a carrying case for the telescope and is used only for transportation. A portable computer to control the system and take the data completes the major components of the lidar. The

computer controls the system using high speed data transfer to various cards mounted in the PC bus. For example, the azimuth and elevation motors are controlled through a card on the PC bus which confers a rapid scanning capability to the system.

A Nd:YAG laser operating at 1.064 microns is used as the laser source. The laser is attached directly to the top of a 25 cm, f/10, Cassegrain telescope. The laser beam is emitted parallel to the telescope after going through a periscope, so that the effective exit aperture is 41 cm from the center of the telescope. The periscope simplifies alignment, and also increases the distance at which the laser beam overlaps the telescope field of view (FOV). This separation decreases the chance of near-field detector overloading, and decreases the dynamic range required of the analog-to-digital conversion system. The telescope-laser system is able to turn rapidly through 210 degrees horizontally and 100 degrees vertically using motors incorporated into the telescope mount.

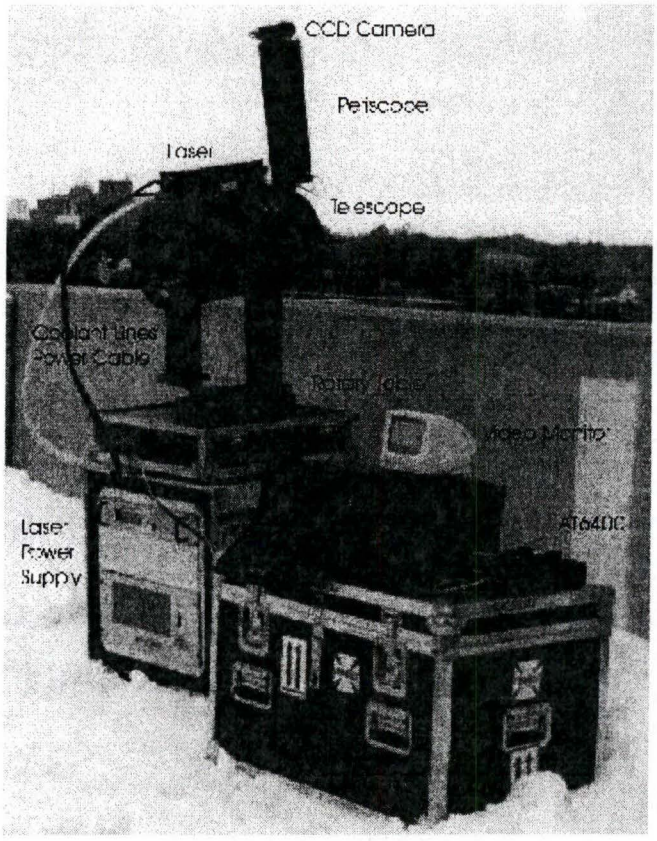

Figure 2: The University of Iowa miniature lidar. The system is designed to be small and portable in order to maximize the number and types of situations in which it may be used..

Behind the telescope, the light passes through the interference filter and a lens system which focuses the light on a 3-mm diameter, IR-enhanced silicon avalanche photodiode (APD). The signal is amplified as part of the detector system and fed to a 12 bit digitizer also on the PC data bus. Two detectors mounted in the periscope sample the outgoing laser pulse and produce signals which are used to correct for pulse-to-pulse variations in the laser energy and

also serve as a timing marker to start the digitization process. Pulse averaging is used to increase the useful range of the system. A series of pulses are summed to make a single scan. A number of scans are used to build up a two-dimensional map of relative atmospheric aerosol concentrations.

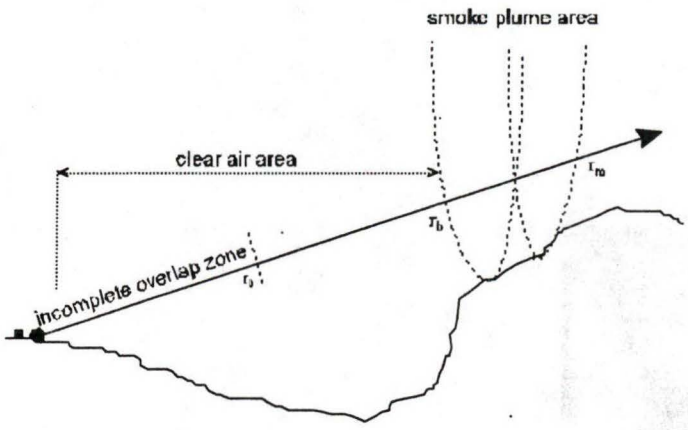

Figure 3: A schematic depiction of the geometry of the demonstration. The lidar was located on the left side on the north facing slope with the fire on the other side of the valley. The nephelometer was located near the lidar. The winds were generally such that the smoke drifted away from the lidar and over the far slope so that the air near the lidar was generally clear.

Normally the lidar is programmed for a series of scans which depend on the area to be scanned. Individual laser pulses can be measured and stored at a frequency of 20-50 Hertz. During each cycle, the lidar will make a series of horizontal or vertical scans which cover the area as well as correlation scans to determine the wind speeds. The operators can quickly change from one scan pattern to another or adjust the number and type of scans to accommodate the particular circumstances. A series of these scans is a cycle. A cycle will take anywhere from seconds to 45 minutes to complete depending on the size of the area to be examined, the resolution of the scans, and the number of laser pulses to be averaged. These cycles are repeated throughout the experiment.

C. Data Collection. The lidar was transported to Montana in anticipation of a prescribed burn site within a reasonable distance from the USDA Forest Service Fire Sciences Laboratory in Missoula, Montana. The dates chosen for observation were the 7th, 8th, and 9th of November, 2001. The experiment was carried out in the mountainous terrain of the Stevensville Ranger District, Bitterroot National Forest, about 10 miles east of Stevensville, Montana. A schematic of the measurement site is shown in Figure 3. The black circular and rectangular labels show the location of the lidar and the nephelometer relative to the burning

area across a small valley. The burn area was on a south facing slope containing grass and pine trees with grass and brush understory. The local winds were light but generally moved smoke away from the lidar and nephelometer location. The lidar was mounted atop a recreational vehicle positioned across a small valley from the site of the burn.

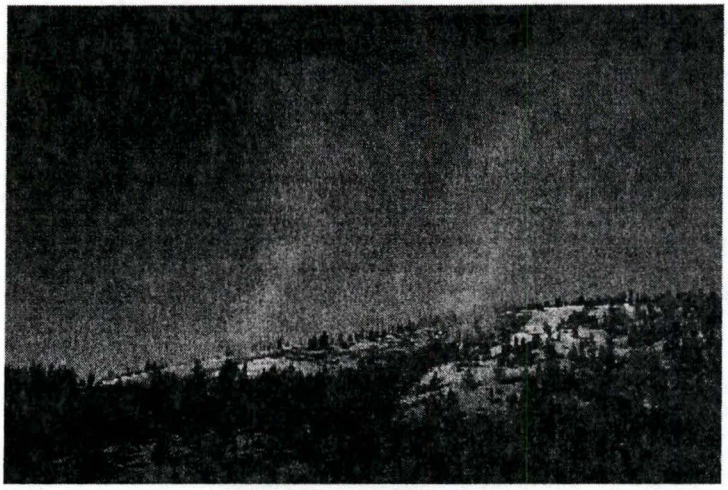

Figure 4: A photograph of the fire shortly after it was started on Wednesday. The fire was confined to the area to the left or downslope side.

The minimum distance from the lidar to the fire was approximately 700 meters. The fire covered an area on the side of the opposite hill approximately 1200 meters across the side of the hill and 300 meters up the side of the hill. Figure 4 is a photograph of the fire about an hour after it was started. The fire on the 8th consisted of smoldering remains from the day before. The fire on Friday, the 9th, was restarted and extended farther down the hill, along the crest on the far side. On all days the fire was on the low end of the range of fire intensity and smoke generation rate typical of prescribed and wild fires.

The files that were taken on the three days are summarized in the appendix. The types of files taken fall into three general categories.

1. Time Domain (TD) Scans. A time domain scan holds the direction of the lidar constant and plots the lidar backscatter (related to the aerosol concentration) along the lidar line of sight with time. This type of scan is most often used for vertical staring lidars and as a lidar diagnostic. It can also be used to derive a number of atmospheric parameters (Eichinger et al., 1993). A TD scan is most effective at showing how the atmosphere is changing with time. The plots are generally simple and easy to understand. A TD plot has time as the x axis and

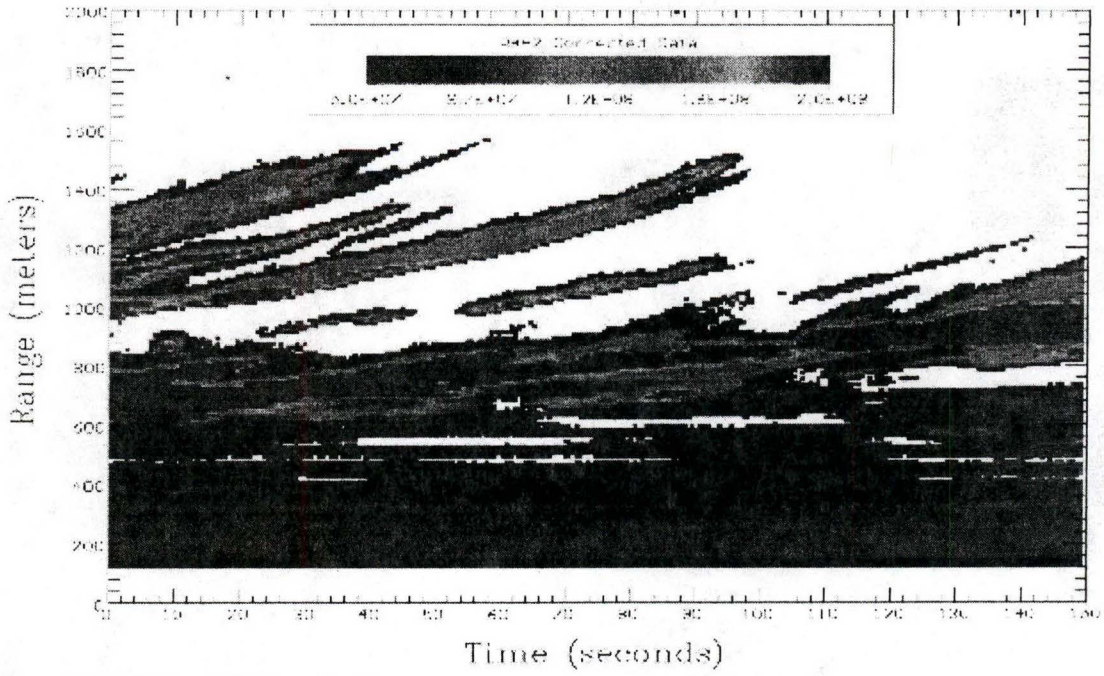

Figure 5a: A TD Scan from November 8.

distance from the lidar as the y axis. The color of the plot indicates the intensity of the lidar backscatter at a given distance and time. Red colors indicate the most intense backscattering and colors tending toward blue indicate less intense levels of backscattering. No color generally indicates a level of backscatter lower than the minimum selected for display.

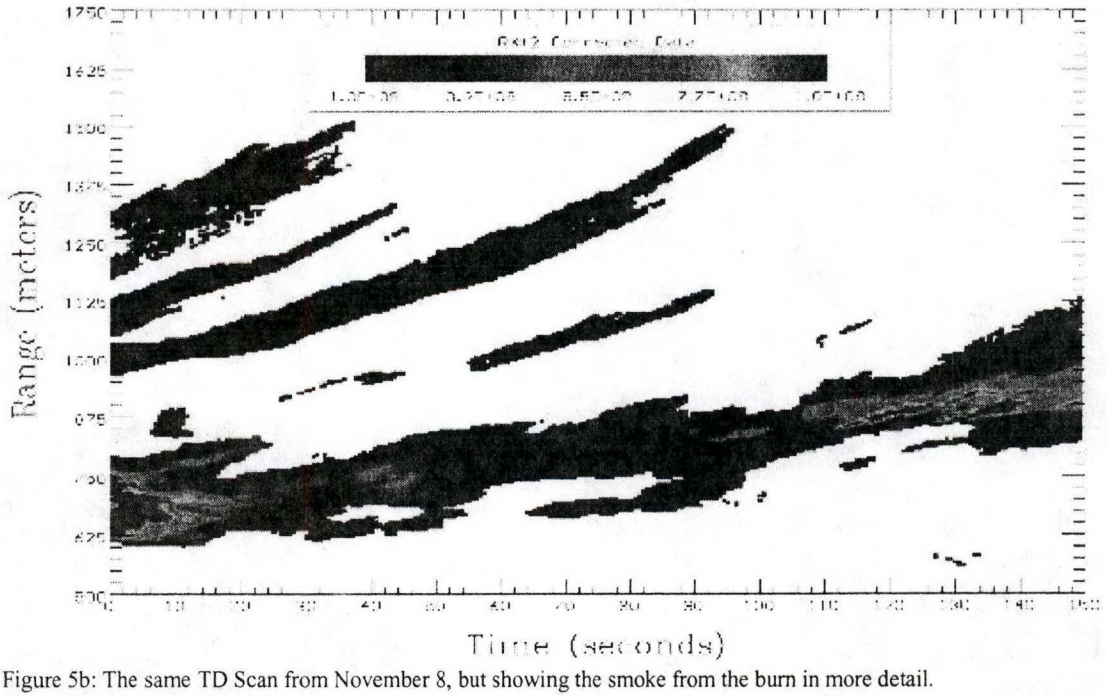

Figure 5b: The same TD Scan from November 8, but showing the smoke from the burn in more detail.

Backscatter intensities greater than the maximum level selected for display are red. The amount of backscatter is proportional to the number density of the particulates responsible for scattering the light (i,e. the amount of smoke in a given area). There are a number of assumptions inherent in this statement that are not generally met, particularly for this application where attenuation of the beam due to the opacity of the smoke is a major issue. However, this statement is useful for interpreting the meaning of the lidar scans. As plotted here, white areas are relatively clean air. Blue areas are moderately contaminated and red areas show the areas of most intense smoke.

Figure 5a,b is an example of a time domain scan above the fire site at an elevation angle of 19 degrees. The first scan, Figure 5a shows the overall scene. On this day, the second day of the burn, the smoke was from smoldering fires from the previous day. Low level smoke filled the lower part of the valley and a limited region near the surface on both sides. Near the lidar, the level of backscatter is higher, due to the residual smoke from the previous days burn, and then decreases as the lidar beam passes through cleaner air above the center of the valley. The smoke from the fires shows up as more intense structures at ranges beyond 600 meters.

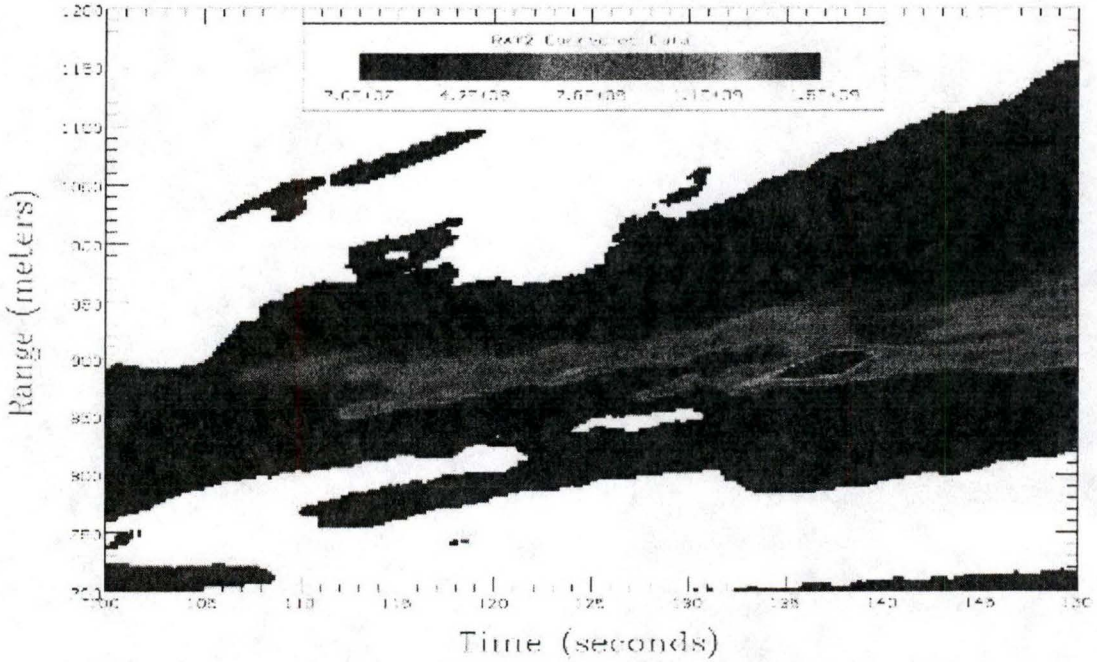

Figure 6: A higher resolution plot of a portion of the TD Scan shown in figure 5.

As the smoke drifts with the wind, it moves away from the lidar, producing streaks in the plot. The component of the wind speed along the line of sight of the lidar is the slope of these streaks. Note that the backscatter from the smoke plumes is more than 100 times more intense than the return from the atmosphere. The level of backscatter from the smoke varies at least a factor of ten. Also of note is the intermittent nature of the smoke clouds at any given range. Figure 5b is a closer view of the smoke plume showing the details of the cloud.

Figure 6 is a plot of the same TD scan in a still higher resolution. This particular scan was taken with 2.5 m range resolution and 0.26 second time resolution. Even simple scans such at this can reveal characteristics of the fire. For example, the green streak from 850 to 950m and 110 to 135s shows multiple puffs of smoke with a regular period of about 5 seconds. Examination of other files shows similar features. Whether this periodic emission of smoke is a characteristic of the smoldering/burning process or is characteristic of turbulent transport is not known.

2. Two Dimensional Scans. Two dimensional scans (2D) fall into two types, horizontal

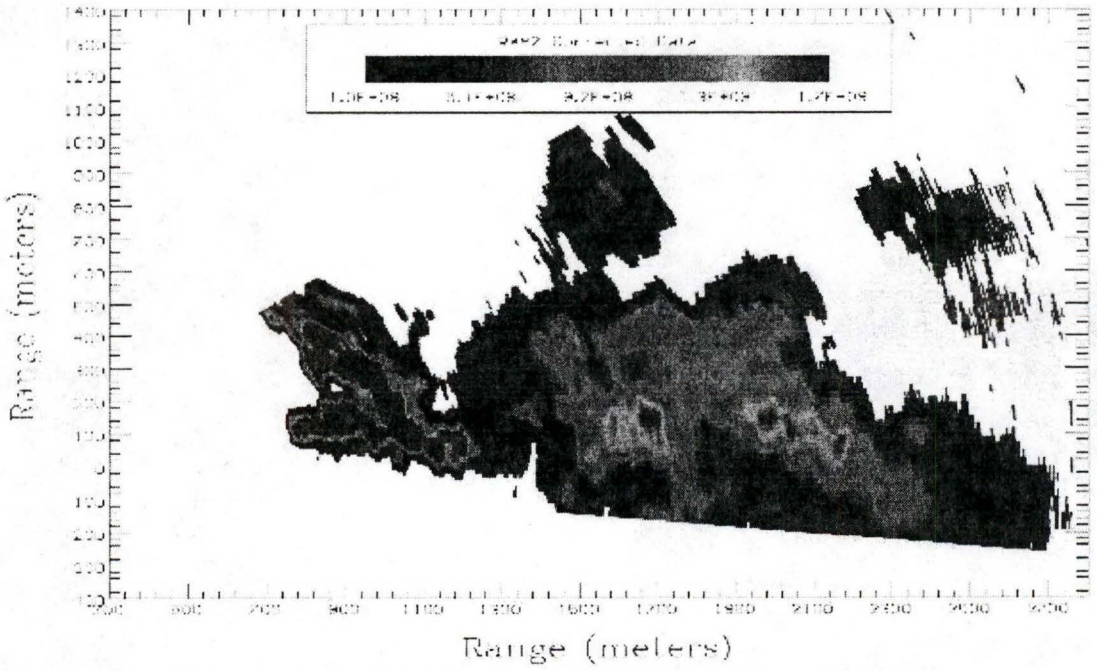

Figure 7: A horizontal scan showing the lidar backscatter from the fire (700 to 1200 m) and from smoke drifting away above the far side ridge (1200 to 2500 m).

scans, showing a slice through the atmosphere at a constant elevation angle and vertical scans, showing a vertical slice through the atmosphere at a constant azimuth. At present, the planes in which the scans can be made have either constant azimuth or elevation. In a horizontal scan, the x axis is the distance from the lidar in the direction 90 degrees clockwise from the lidar default direction. The y axis is the distance from the lidar along the default direction. Thus, to make the scan shown in figure 7, the lidar scanned the region to the right of its default direction.

Figure 7 is an example of a horizontal scan data plot at an elevation angle of 20 degrees. This angle creates a plane just above the hill and the trees on it. Rising smoke from the fire is transported through this plane. Laser light that is reflected from this smoke is detected by the lidar. Smoke from the fire can be seen as the red area between 700 and 1200 m. More diffuse smoke can be seen farther away and downwind. This type of scan is useful to delimit the area in which fires exist. While this scan was made only in that part of the hill that was being burned, the region of the hill that is burning is clearly seen to be well-defined. In other words, scans of this type could be used to estimate the size of the burning region. The degree to which the burning area can be accurately estimated will depend on how close to the surface the lidar

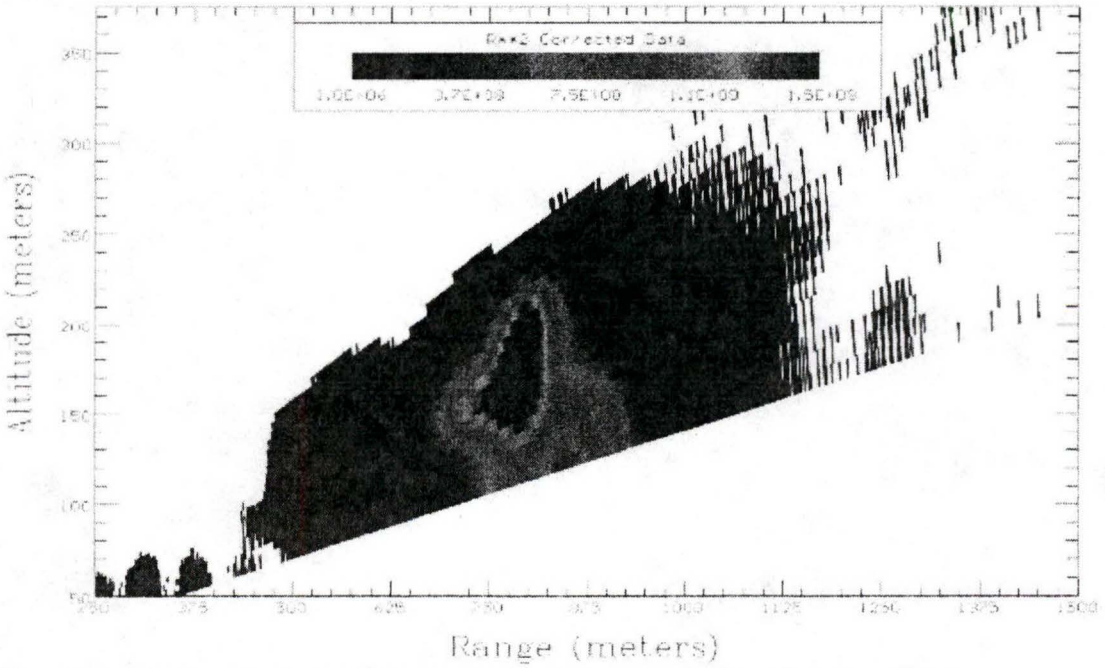

Figure 8: A vertical scan showing the lidar backscatter from the smoke from fires on the last day. This scan is made at a wavelength of 532 nm.

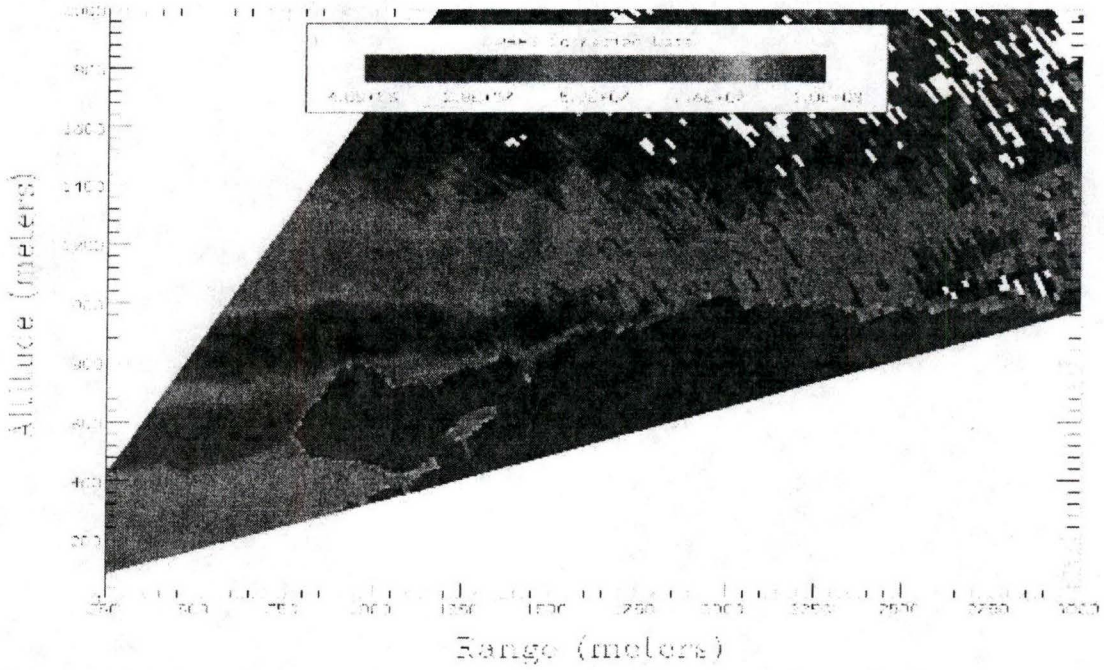

Figure 9a: A vertical scan showing the lidar backscatter from the residual smoke from the day's burning along with an intense area filled with smoke. The residual smoke is seen as green areas below 400 m, at about 700 m, and from 1000 to 1400 m. The scan is directed across the valley toward the fire.

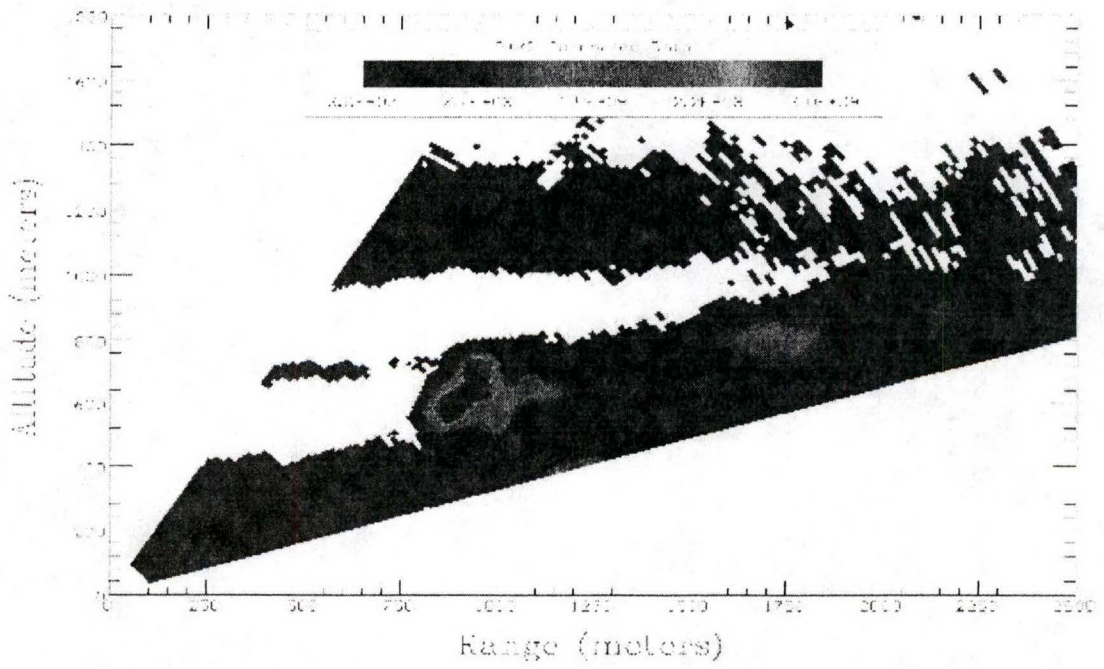

Figure 9b: A same vertical scan shown in figure 8a, but with a different color scale in order to show details of the smoke cloud.

can scan. Since the smoke diffuses with altitude the estimate will be more accurate as the scan is performed at lower altitudes.

Figure 8 is an example of a vertical scan data plot directed across the valley on the last day. In a vertical scan plot, the x axis is the horizontal distance from the lidar. The y axis is the distance above or below the lidar location (which is taken as zero elevation). Figures 9a and 9b show a vertical scan of the smoke cloud. This scan was taken late in the day when a small amount of smoke haze existed in the valley. It can be seen in figure 9a as three horizontal green bands. This late in the day, a stable atmospheric condition was setting up in the valley, causing the layering. The top of the day's boundary layer can be seen at about 1400 m (above the lidar). The air above this level is cleaner than the air below. Figure 9b is the same scan, but with a different color scale to bring out the variations in the smoke plume itself. Note that the two color scales span a range of backscatter intensities of about 1000, from the clear sky to the most intense part of the smoke plume.

3. Correlation Scans. A correlation scan is similar to several time domain scans in different directions made simultaneously. The lidar is commanded to average the

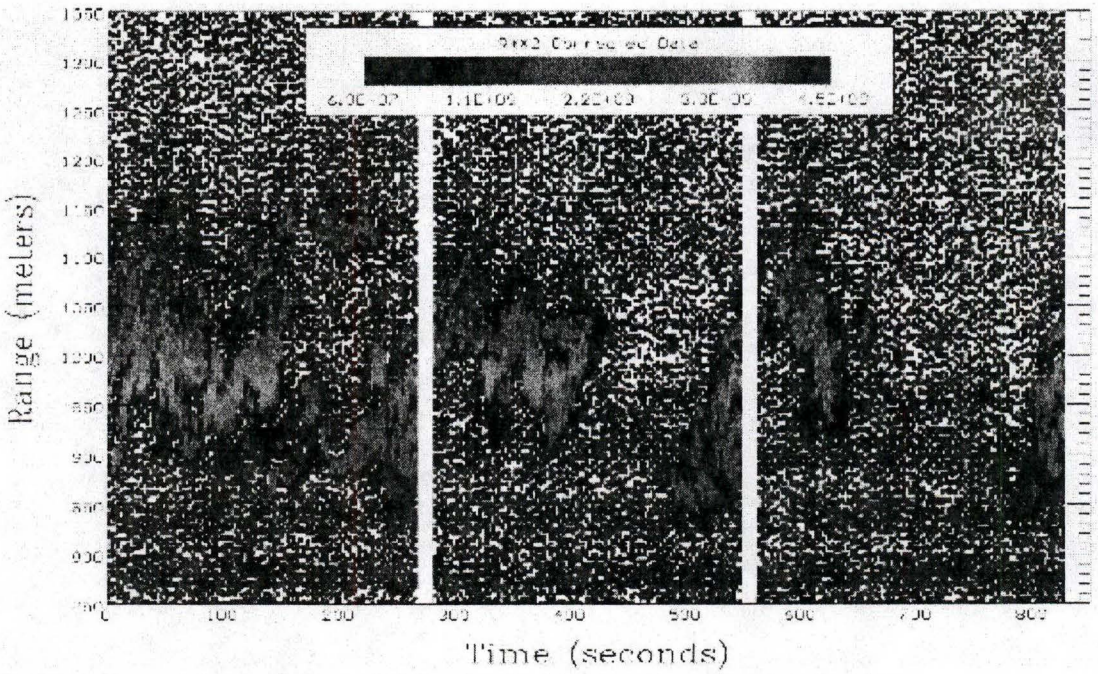

Figure 10a: A correlation scan in the vertical direction showing the smoke concentration along three different lines of sight oriented above one another. The left panel is the lowest altitude, the right panel is the highest.

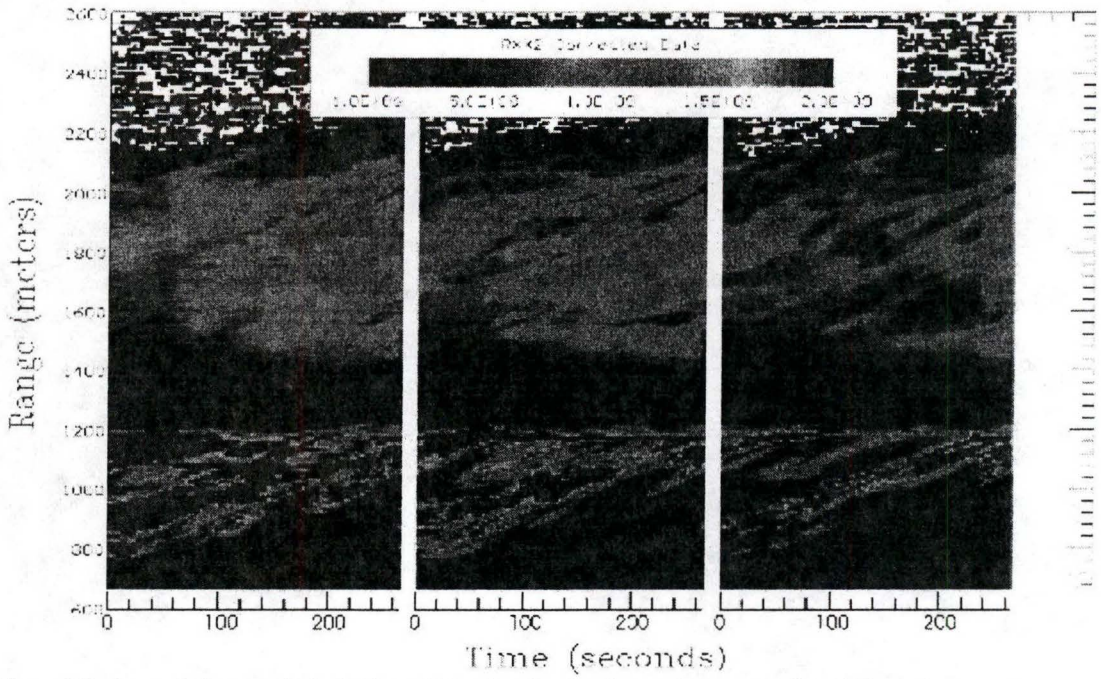

Figure 10b: A correlation scan in the horizontal direction showing the smoke concentration along three different lines of sight oriented along side one another. The left panel is made at an angle to the left of the others, the right panel is made at the rightmost angle.

return from a given number of laser pulses in a given direction, then move to another direction and average the return from the same number of laser pulses. The number of directions at which this is done is user selectable. Once the desired number of directions is sampled, the scan repeats this process a desired number of times. The result is several TD scans that are slightly different in appearance. Figures 10a and 10b are examples of a correlation scan in the vertical direction and the horizontal direction. A correlation scan in the horizontal direction is perhaps easiest to interpret. For the case of figure 10b, the wind was moving away from the lidar and to the right. The scan represents three lines of sight through which the smoke plumes will pass. In this case, a portion of the plume will pass through the leftmost line of sight first, then through the middle line of sight at a later time, and through the rightmost last. Because there is a component of the wind velocity along the line of sight, that portion of the plume will also enter the other lines of sight at different distances from the lidar. Thus, the three images will be similar, but shifted slightly in space and time. The size of the shifts can be used to determine the wind speed and direction. Note that the smoke plumes diffuse as they move, so the

intensity of the lidar backscatter decreases with time (i.e. the backscatter intensity in the right panel is significantly lower than it is in the left panel).

Prior to this demonstration, the lines of sight were limited to different azimuths at the same elevation angle. The ability to make correlation scans at constant azimuth angle and different elevation angles was added for this demonstration. Figure 10a is an example of such a scan. It was believed that a lidar multi-angle inversion routine could be performed on the data in order to obtain high quality attenuation coefficients.

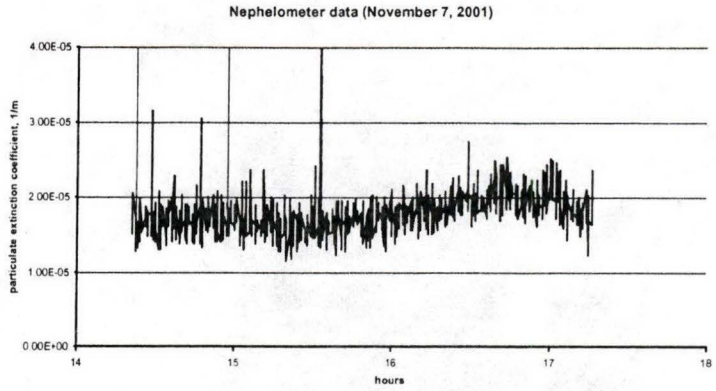

Figure 11a: Nephelometer measured particulate extinction coefficients on 7 November.

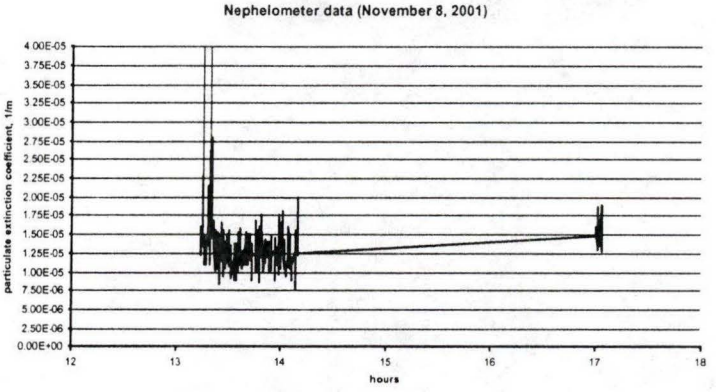

Figure 11b: Nephelometer measured particulate extinction coefficients on 8 November.

D. Nephelometer. A nephelometer is an instrument in which a small volume of the ambient air is illuminated by a narrow beam of light. A photoreceiver inside the instrument measures the intensity of light scattered inside the

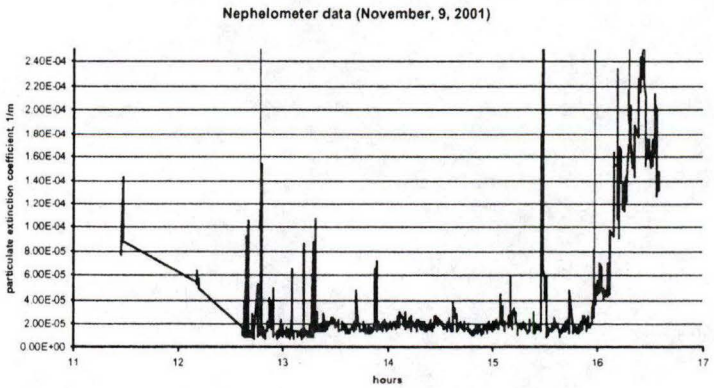

Figure 11c: Nephelometer measured particulate extinction coefficients on 9 November.

volume, at angles shifted relative to the direction of the incident light beam. The amount of scattered light measured by the photodetector is related to the turbidity of the ambient air. There is a correlation between the intensity of the angular scattering and the extinction coefficient inside the scattering volume. There are four basic types of nephelometers that are in common use: (1) a side-scattering nephelometer; (2) an integrating nephelometer; (3) a forward-scattering instrument, in which the scattering angle is close to zero, and (4) a backscattered light nephelometer, in which the scattering angle is close to 180^0. This instrument operates accurately only within a relatively limited range of visibilities. However, the use of a nephelometer is the only practical method for visibility measurements in weather conditions where the opacity of the atmosphere is high.

The components of a nephelometer are not spatially separated and is generally constructed as a single unit. There are several basic assumptions that are made which also limit nephelometer measurement accuracy. First, it is assumed that the total extinction coefficient of the atmosphere is strictly related to the scattering at a particular angle in a small scattering volume. Second, this relationship is assumed to be known or may be experimentally established during a preliminary calibration procedure. Third, this relationship is assumed to be the same for different types of atmospheric situations. This means that for any given visual range, no variation in the particulate size distribution or in the index of refraction will vary the angular intensity of the scattered light. The small scattering volume is also a disadvantage of these instruments and may result in large fluctuations in the measured signal and large measurement uncertainties, especially, in changing atmospheres.

In spite of these limitations, a nephelometer is easy to set up and can provide a known particulate extinction value in a location that the lidar and reach. This is an important additional piece of information that can enable far more accurate inversions. In this demonstration, the nephelometer was placed near the lidar so that it might measure the particulate extinction coefficient of the clean air. Because of the geometry of the experimental site, siting the nephelometer in the valley between the lidar and the fire was impossible. A Radiance Research model M903 nephelometer operating at 530 nm was set up upwind of the lidar location.

Figures 11 a, b and c show the nephelometer data. Note that the clean air in the valley maintained an particulate extinction coefficient of about $2x10^{-5}$ on all three days except for the last two hours and several short episodes. For comparison purposes, this is approximately one-tenth of "normal" sea level air [Measures, 1984].

E. Data Issues.

1. Contrast. This issue of the large difference between the backscatter coefficients for the ambient air and the smoke plume is perhaps the most significant problem in developing a lidar system for use in forest fire measurements. As can be seen in figure 12a, the difference in backscatter intensity in the smoke cloud is more than a factor of ten. The difference in backscatter intensity between the cloud and the ambient air can be seen in figure 12b to be more than 400.

The difference in backscatter intensity is important because a given digitizer has a finite dynamic range. For a 12 bit digitizer, there are 4096 (2^{12}) gradations between the largest and smallest voltage that can be measured. At the time of writing, 12 bit digitizers operating at

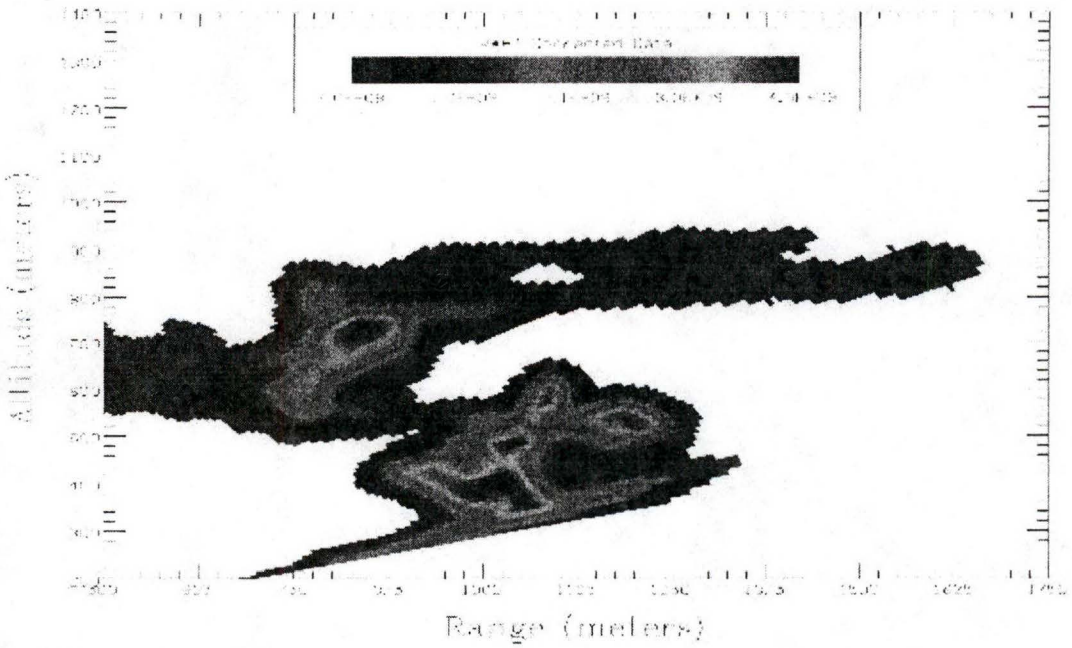

Figure 12a: A vertical scan showing the details of the smoke plume over the fire during the first day. The color set has been adjusted to show just the region contaminated by smoke from the fire.

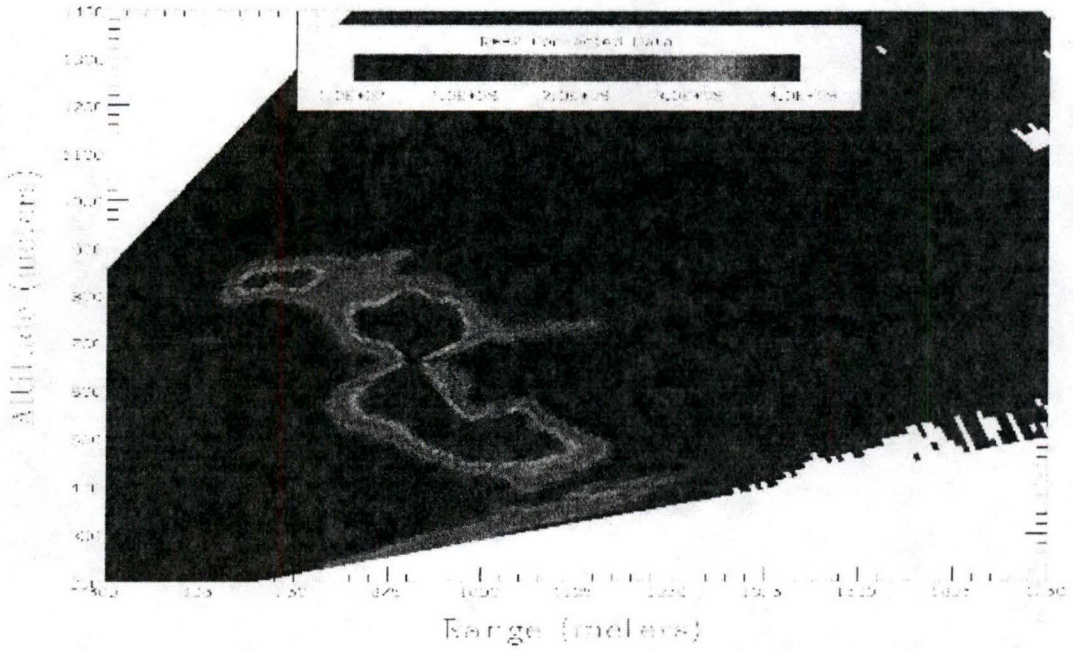

Figure 12b: A vertical scan showing the smoke plume over the fire from a time just previous to the data in 10a. The color set has been adjusted to show both the ambient air and the region contaminated by smoke from the fire.

approximately 100 MHz are the state of the art. Faster digitizers are available, but in less depth (i.e. 8 bit digitizers). Deeper (14 or 16 bit) digitizers are available, but at slower digitization rates (usually below 10 MHz). One manufacturer (Gage) has just released a 14 bit, 100 MHz digitizer, but it is not yet in common use. In the discussion to follow, it is assumed that the lidar signal is amplified to optimally fit the voltage range of the digitizer, and that the digitizer offset is fairly small. While this is not difficult to accomplish, to do so for a long period of time or under varying conditions requires constant attention to the signal and changing the data collection parameters (for example the laser power, the detector APD bias, or the detector amplification). Changing the data collection parameters may not be desirable depending on whether the system is calibrated or not, or may affect the linearity of the electronic response.

When processing lidar signals, it is desirable to have data on the ambient air on both sides of the atmospheric structure of interest, in this case, the smoke cloud. Figure 13a is an example of a single line of sight from the two-dimensional scan in figure 12b. The signal from the plume reaches to near the maximum level obtainable by the digitizer (4095). The signal from ambient air can be seen on both sides of the plume. The backscatter intensity is as much

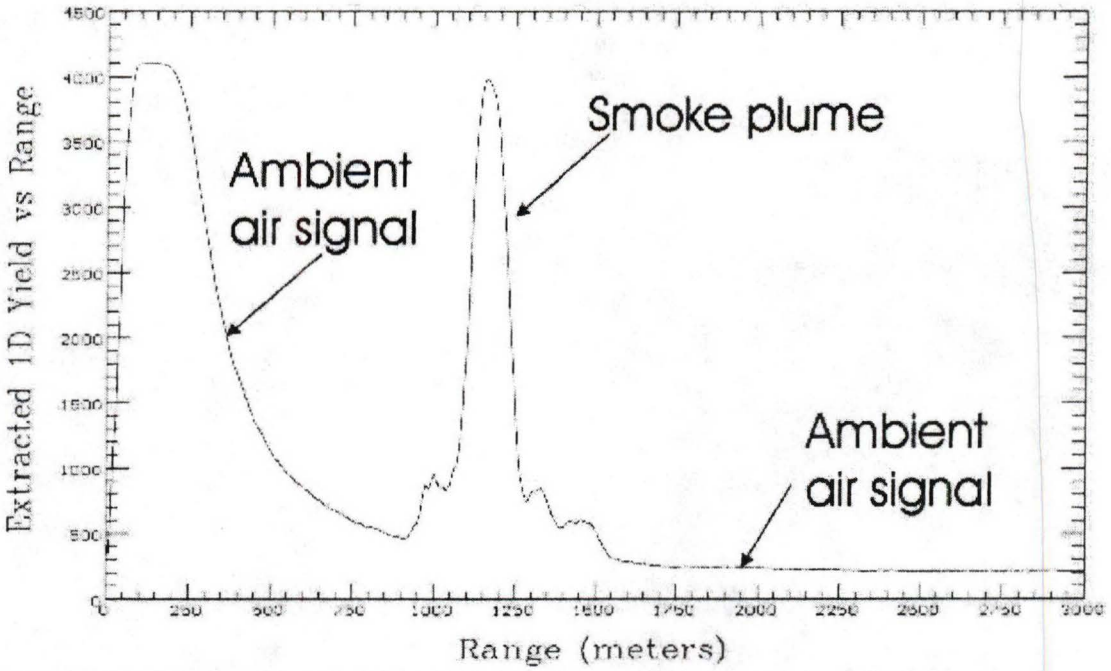

Figure 13a: The lidar signal from a single line of sight (37.5 degrees elevation) from the two dimensional scan shown as figure 11b.

as one-hundred times that of ambient air (4000 at the peak vs 400 at the base). It would appear that this signal is well-adjusted for the situation. However, an examination of figure 13b shows that the signal to noise ratio for the ambient air on the far side of the plume is rather poor.

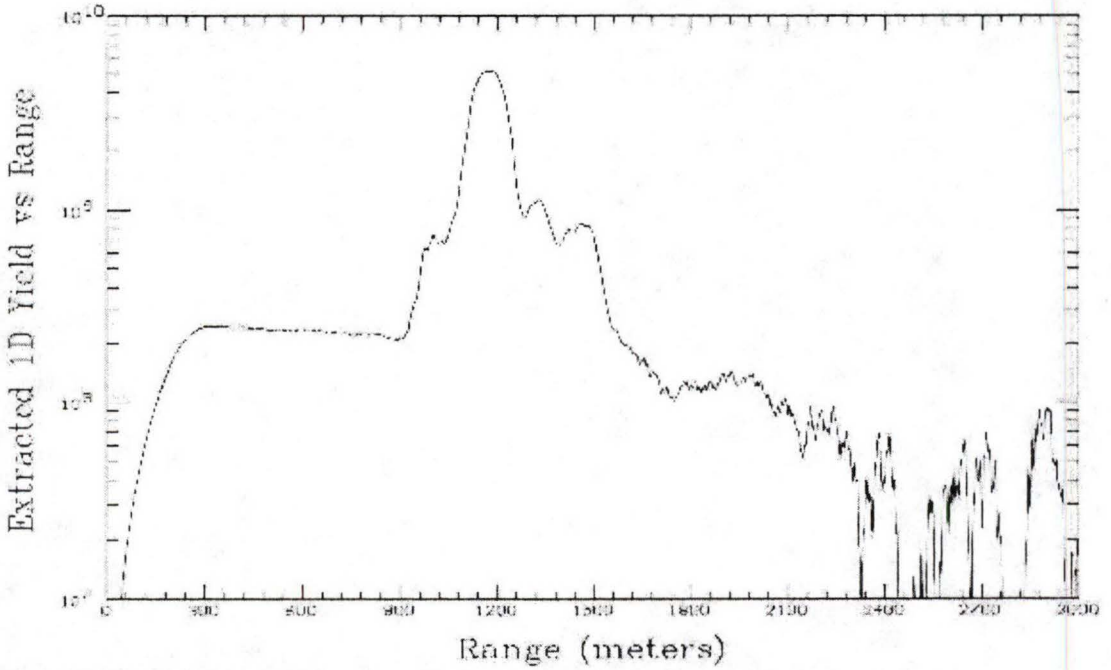

Figure 13b: The same lidar signal from figure 13a, but corrected for the attenuation due to range.

The ambient noise level is approximately 25 units, so the signal to noise ratio is only about ten at 2000 m and continues to decrease as the range increases. The maximum signal to noise is then about 150.

The problem is that to obtain a better signal to noise ratio in the far field would require an increased signal level from these ranges. This would however, raise the level of the signal from the smoke cloud to a level higher than could be measured by a single digitizer. If this happened, no data could be obtained from this area, and would greatly complicate efforts to invert the signal.

2. Different Wavelengths. The use of different wavelengths is one possible approach to the problem of contrast. As wavelengths become longer, the lidar response is less affected by molecular scattering (molecular scattering cross sections are proportional to wavelength^{-4}) and more sensitive to particulate scattering (particulate scattering cross sections are approximately proportional to wavelength^{2} for particulates small with respect to the laser wavelength). Thus by moving from the Nd:YAG fundamental at 1064 nm to the frequency

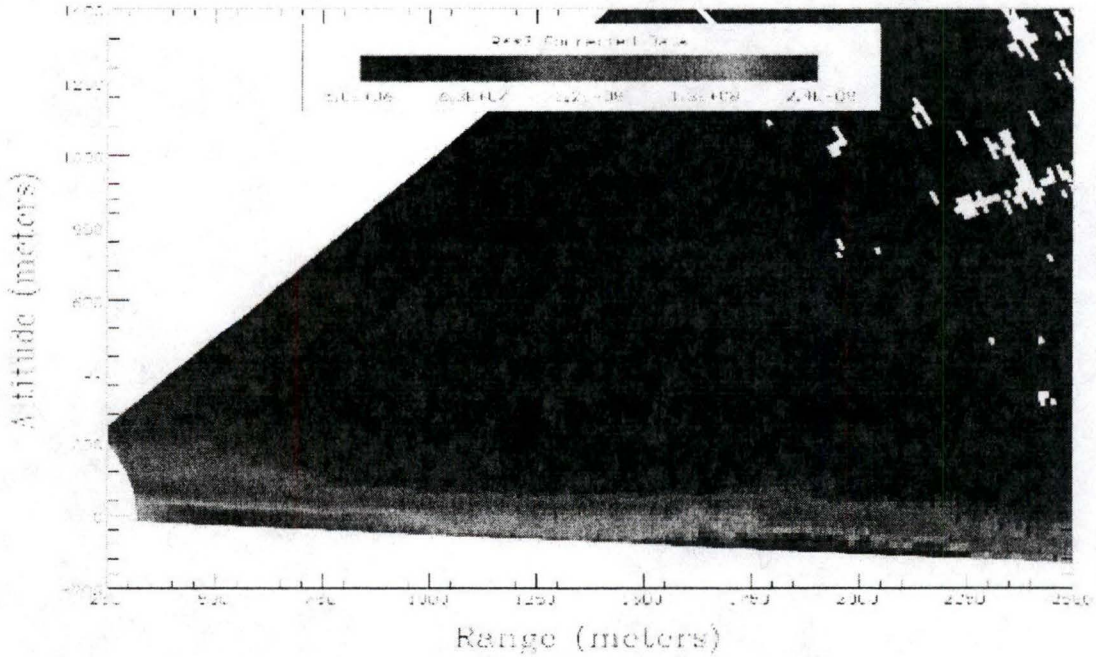

Figure 14a: A 2D vertical scan looking down the valley between the lidar and the fire. The red color at lower levels is due to the smoke and haze from two days of burning

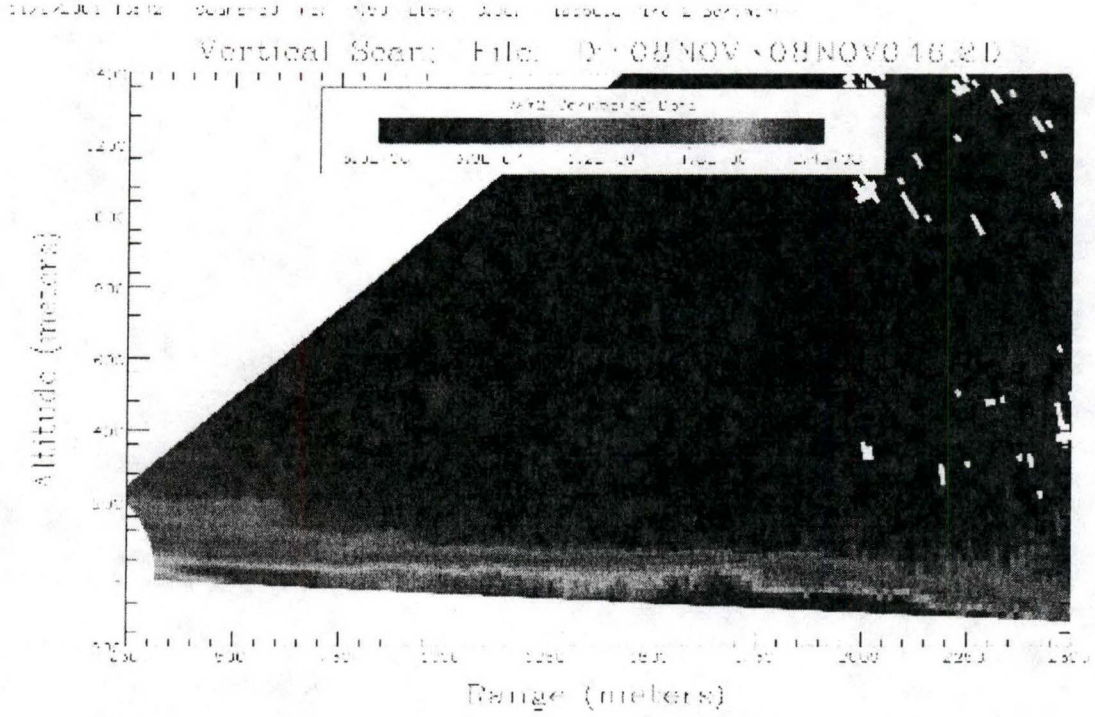

Figure 14b: The same view as in figure 14a, but at a later time.

doubled wavelength at 532 nm, one changes the relative scattering by a factor of about 2^6 or 64. Changing to a wavelength of 355 nm (frequency tripled Nd:YAG) will change the relative scattering by a factor of 3^6 or nearly 900.

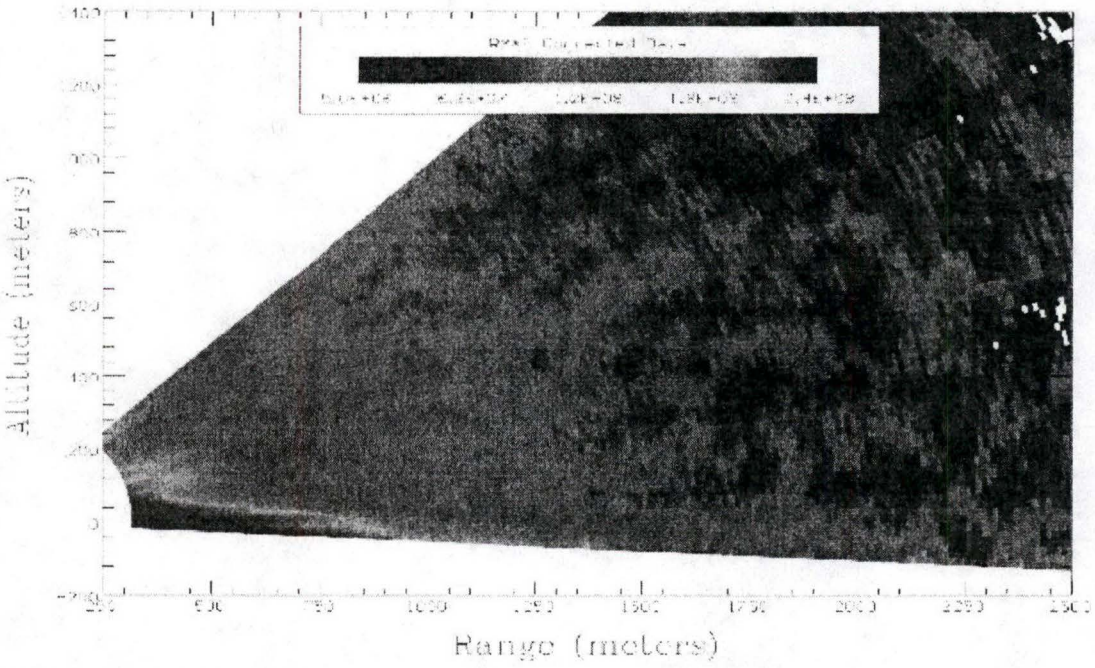

Figure 15a: The same view as shown in figure 14 except made with 532 nm laser light.

Figure 14a and 14b are examples of vertical scans using a laser wavelength of 1064 nm. Figure 14a is taken in the direction of the "clean" air down the valley center. The higher smoke levels below level of the lidar are the result of smoke from the previous day's fires, but appeared to the eye as being clear. Smoke from the previous day's fires and captured by the stable atmospheric conditions, settles in the lower part of the valley and in the region near the hillsides. The lidar sees this residual smoke as a higher backscatter (the red in the lower part of the scan) and the cleaner air above (the green and blue color). The increase in the level of backscatter near the ground at this time can be seen in the increase in extinction coefficient in figure 11c at the end of the day.

Contrast these figures with figure 15a showing the same "clean" air down the valley but at 532 nm. A big difference between figures 14a and 15a is the attenuation of the signal in figure 15a. The colors in the plot at an altitude of 400 m, for example, decrease from greens to blues as one moves away from the lidar. The attenuation can be compensated to some degree

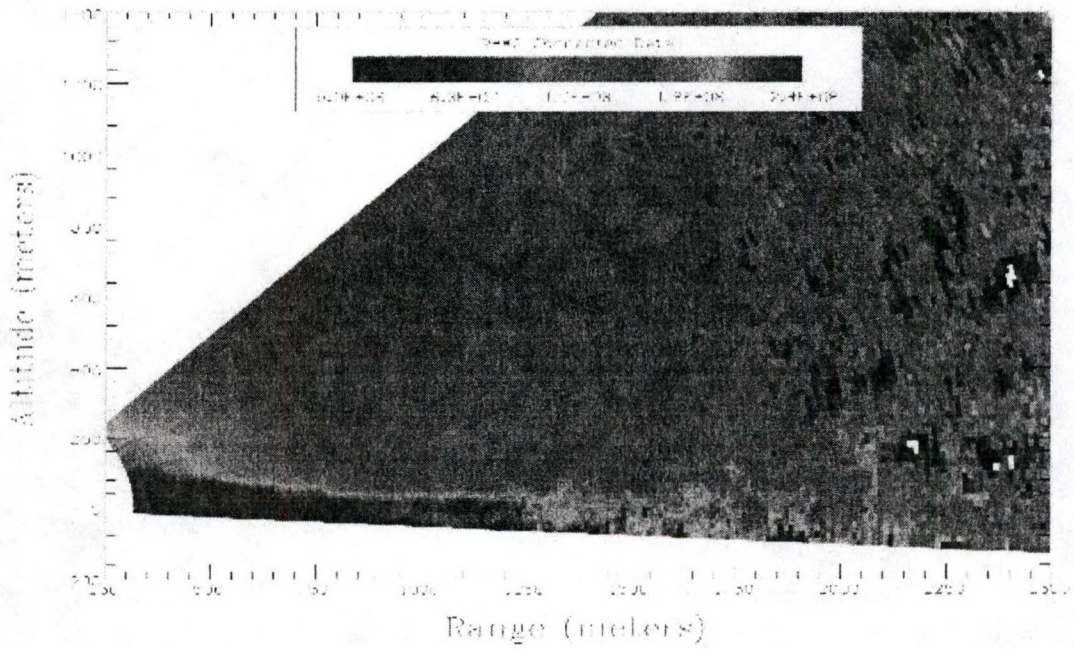

Figure 15b: The same data as shown in figure 15a, but corrected for large scale attenuation. The correction is made by determining the average attenuation of the lidar signal by the slope method.

(accomplished here as the removal of the average attenuation determined by a slope method)

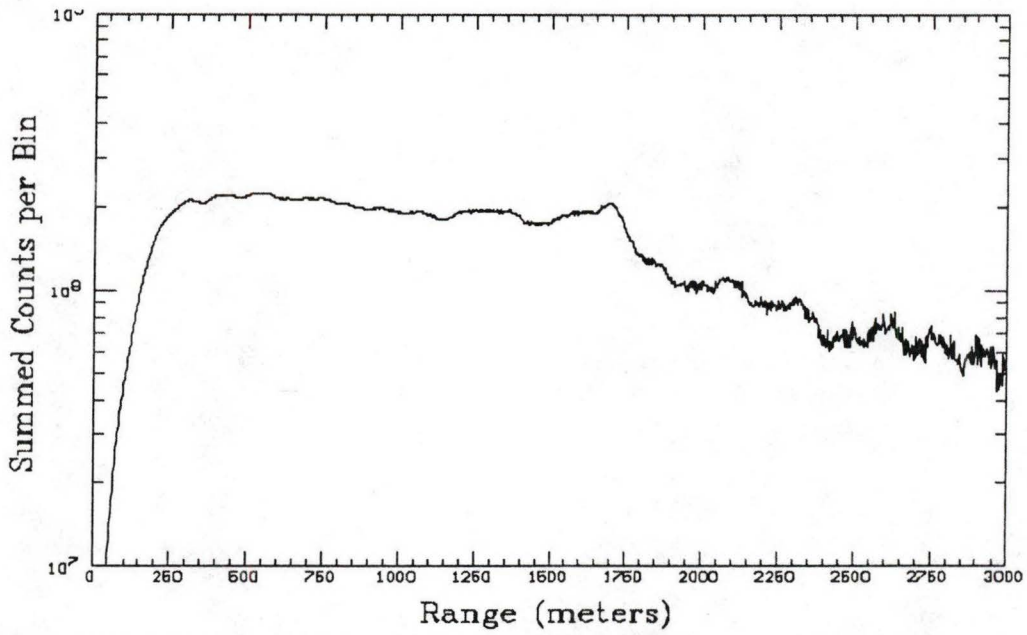

Figure 16a: The lidar signal from a single line of sight at zero elevation using 1064 nm laser light. The data is taken from the same set as figure 14.

as can be seen in figure 15b, but does not restore the signal quality to the same degree as that in the 1064 nm signal (figure 14a) at long ranges (compare, for example, the signal at 2000 m at the lidar level in both figures). This situation represents one extreme at which the use of multiple wavelengths can be compared. For the case of relatively clear air, as here, the use of a longer wavelength will enable the detection of low levels of particulates at longer ranges. This is due to the increased sensitivity to particulate scattering and the decreased attenuation at longer wavelengths.

The differences between the two wavelengths can be seen in figures 16a and 16b. These are the range-corrected lidar returns from zero elevation and an average of 1000 laser pulses. The most prominent difference between the two is the decrease in the signal with distance. In both cases, the laser beam exits the more contaminated area at a distance of 1500 to 1700 m. This is clearly seen in the 1064 nm data as a small increase then a rapid drop in the signal in this region and beyond. Above this layer, the particulate density decreases with altitude and the signal decreases proportionately. The same structure can be seen in both plots

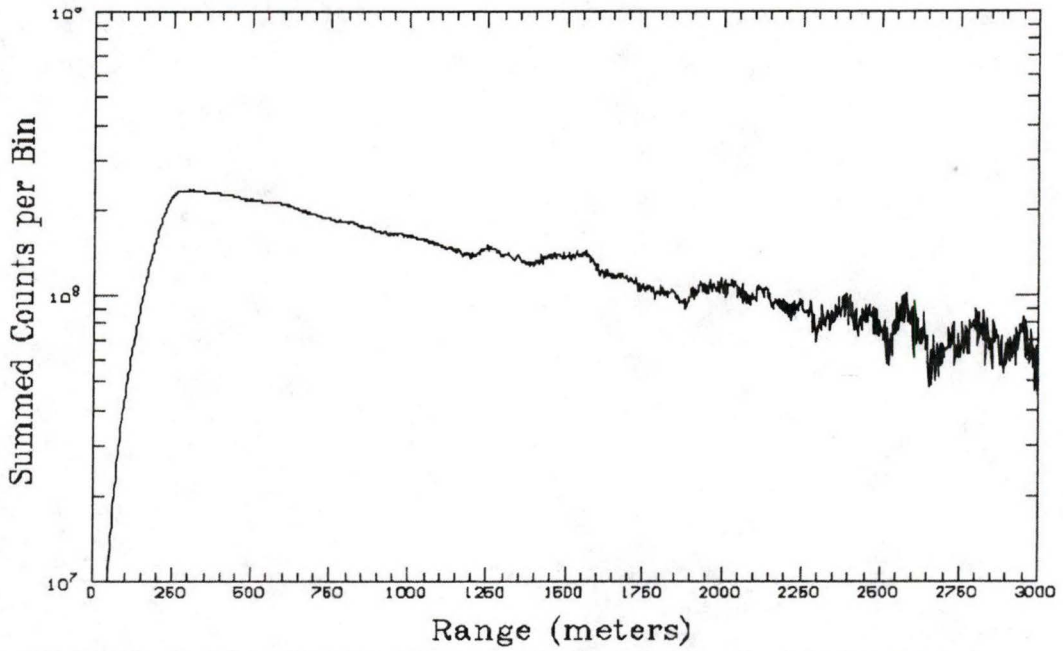

Figure 16b: The lidar signal from a single line of sight at zero elevation using 532 nm laser light. The data is taken from the same set as figure 15.

at approximately 1500 m, however, it is much less prominent in the 532 nm data. In addition, the decrease in signal as the beam exits the boundary layer is much smaller for the 532 nm data. This confirms the statement that the contrast is significantly reduced for shorter wavelengths between the particulate scattering in clear air outside the smoke plumes and that inside the smoke plumes.

The level of ambient sunlight is significantly different for these two wavelengths. 532 nm is very near the peak of the solar spectrum. In contrast, the amount of sunlight is significantly decreased at wavelengths of 355 nm and 1064 nm. However, the level of light scattered by the atmosphere is greater at 355 nm (and thus the clear sky background signal) than it is at longer wavelengths. The amount of background light sets a lower limit on the signal to noise ratio, and also sets a limit to the maximum amplification that can be obtained from the detector.

3. Angled Scans. For most common lidar work, the desired measurement geometry is

primarily rectangular and oriented with respect to the vertical direction. Thus horizontal scans, for example, are made at constant elevation and in planes that are perpendicular to the vertical. It was clear during the demonstration that this type of scanning strategy is less than optimal for rugged terrain. A better type of scan than the current horizontal scan would be one that was parallel to the surface slope. This could be done by progressively changing the elevation angle as well as the azimuth angle as the scan is made.

III. DISCUSSION / CONCLUSIONS

Several conclusions can be made with respect to the demonstration. Lidars are manifestly capable of making the kind of measurements needed to estimate the emission rate, at least from modestly sized forest fires. However, the method is not without limitations that must be addressed to be an effective tool for this purpose.

A. Dynamic Range. This problem is arguably the most important issue to be solved and is particularly difficult because of the wide range in backscatter coefficients found in smoke clouds (factors of 10 to 100 at 1064 nm) and the large difference between the backscatter coefficients of smoke clouds and that of ambient air (factors of 50 to 1000 at 1064 nm). In order to invert the lidar data (at least using current techniques), the entire range of reflectivities must be detectable by the lidar.

The use of shorter wavelengths is preferable to the Nd:YAG fundamental at 1064 nm that is the primary wavelength of the UI lidar. This will limit the dynamic range of the data for inversion purposes, facilitate calibration of the lidar , and if the wavelength is shifted to UV, will make it easier solving the eye-safety problem. However, a better solution may be to use multiple wavelengths. This would maintain the sensitivity to low particulate concentrations and longer range offered by long wavelengths while obtaining more compressed dynamic range from the shorter wavelength. Data analysis could be done using the two data sets together, one to obtain cleaner air attenuation coefficients that could be used on the other data set. One issue that must be addressed is eye-safety at shorter wavelengths. The frequency doubled Nd:YAG

wavelength is at 532 nm, a wavelength to which the eye is quite sensitive and that is well-focused by the eye, making it particularly dangerous to use. The frequency tripled wavelength is at 355 nm, which is invisible to the eye and has a considerably lower damage threshold.

The use of multiple digitizers is another possible approach to the dynamic range issue. The idea is to use one digitizer to measure large reflectivities and one to measure an amplified signal so as to detect much smaller reflectivities. This will improve the situation to some extent, but relies extensively on the dynamic range of the detector and preamplifier. At some point, the signal will decrease to the point where it is comparable to the electronic noise, at which point no amount of amplification will help. The largest signal to noise claimed by any manufacturer is 10^4 (Licel), although data provided by the manufacturer indicates that it is significantly less. However, this is not sufficient dynamic range for this application. There is also the question of the degree of linearity over this range of values. Because of this, another possible solution is the use of two detectors at a given wavelength. One would be adjusted, either electrically or optically, to detect the signal from intense backscattering, and one would be adjusted to detect the ambient air. Each detector would have its own digitizer so that between the two detector/amplifier/digitizer systems, there would be sufficient dynamic range to meet the need. A dynamic range greater than 10^4 could be obtained for high quality data with signal to noise ratios greater than about 50. This option is difficult to implement for a small scanning lidar of this type, particularly if multiple wavelengths are used, because of the size and weight of the detector system.

B. Inversion Methods. The development of inversion techniques for a two component atmosphere or in this case a three component atmosphere (clean air, somewhat contaminated air, and intense smoke plumes) with large differences in opacity is needed. To our knowledge, none of the existing lidar-equation solutions are suitable to determine the extinction coefficient for smoke particulates. The conventional methods used to determine the boundary conditions, such as those used in Klett's far-end solution [Klett, 1981], the optical depth solution [Kunz, 1996; Marenco et al., 1997], or the assumption of an aerosol-free

atmosphere [Sassen and Cho, 1992] are not practical when examining smoke from biomass fires. An additional problem that significantly exacerbates the processing of such signals, is the enormous difference between the backscatter signal intensity from distant smoke and that from adjacent clear air. The backscatter signal from clear air beyond distant smoke plumes usually has a poor signal-to-noise ratio and cannot be used as a reference data point. Lidar signal inversions are further complicated by the uncertainty in the backscatter-to-extinction ratio of the smoke particles, and the presence of a multiple-scattering component in the backscatter signal, at least when measuring dense smoke.

When measuring the optical properties of aerosol particulates with lidar, independent reference data, for example, obtained with a nephelometer, may be helpful to establish a measured boundary condition, *a priori* that may be applied to the inversion. However, the practical application of this data, obtained at the lidar measurement site, might be problematic when using the conventional lidar near-end boundary solution, which is known to be unstable.

Kovalev [2002] has been working on an inversion algorithm based on near-end reference data obtained with a nephelometer. This method is a combination of conventional boundary point and optical depth solutions that may be practical in this kind of situation. This inversion method is a modified form of the optical-depth solutions developed by Weinman [1988] and Kovalev [1995]. The value of the combined inversion algorithm is corroborated by experimental data obtained during prescribed fires and numerical simulations [Kovalev et al., 2002a].

C. Improved Signal-to-Noise Ratio. In order to obtain a reliable inversion, it is desirable to have a maximum signal-to-noise value greater than 1000 [Kunz and Leeuw, 1993]. The data obtained during this demonstration has a maximum signal-to-noise of about 200. Figure 17 is a sample of a single line of sight, in the region of the peak, from a vertical scan through relatively clean air. The signal is the average from 50 laser pulses, has been background subtracted, range corrected, and smoothed using a five point, two dimensional smoothing routine. The variations in the signal have a magnitude of slightly less than 4×10^5,

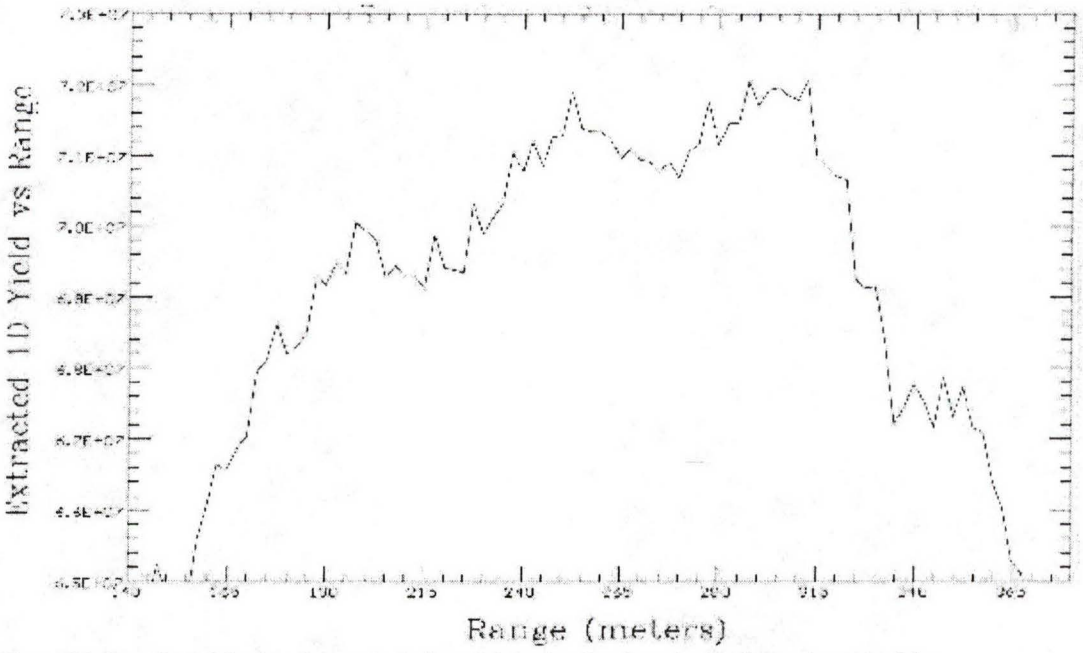

Figure 17: A portion of the data from a single line of sight showing the noise level near the peak of the signal.

measured peak to peak. With a maximum signal of just over $7x10^7$, the maximum signal-to-noise ratio is about 200.

This relatively low signal-to-noise ratio is in part due to an error made during the demonstration. Anticipating that dynamic range was going to be an issue, the high voltage bias on the silicon APD was reduced to the minimum level that would maintain linearity in the detected signal. The laser voltage supplied to the flashlamps was also reduced to the lowest value consistent with uniform lamp firing (i.e. the laser energy would stay constant from pulse to pulse). Any loss in signal amplitude in the near field was then made up by increasing the gain in the digitizer. In retrospect, this was a mistake in that it reduced the lower noise gain in the APD to nothing while retaining all of the natural noise sources in the detector/amplifier combination. What should have been done is to maintain the APD voltage to obtain a higher signal-to-noise ratio and further decrease the laser power. The laser power could have been further decreased by increasing the time delay of the q-switch. A detailed examination of the data was not made during the demonstration, so the low signal-to-noise was not addressed at the time.

Since the time of the demonstration, several improvements have been made to the system that impact on the signal-to-noise ratio. The first is the use of a thermo-electrically

cooled detector/amplifier combination. This drastically increases the signal-to-noise ratio by a factor of about 20 to 50 over the detector/amplifier used in the demonstration. The second is a wavelet routine that removes the "ringing" in the near field caused by the flashlamp firing. This enables us to use the data much closer to the lidar.

D. Development of Slant Scanning Techniques. As stated previously, the experience gained during the demonstration indicates that the ability to adjust the orientation of the scans to the terrain would be helpful. Work has begun on developing a slant scan to replace the current horizontal scan made at a constant elevation. The development of a three dimensional scan of this type is being considered. In addition to solving the problem of how to take such a scan, the current configuration of the program is not set up to handle this many scanning parameters. The problem is to implement this type of procedure while maintaining backwards compatibility.

E. Vertical Correlation Scans. The vertical correlation scans were made with the anticipation that one or more of the conventional multiangle inversion routines could be applied to them. These routines assume a uniform atmosphere, at least in horizontal directions. They might be applied well to this type of scan in some clear atmospheres (Porter et.al, 2000; Sicard et. al, 2002), or under conditions of perhaps fogs or low clouds where horizontal homogeneity is found (Rybakov et. al, 1991). However, the plumes of smoke from the fires show large variations in intensity over short distances and times. They do not meet the conventional criteria for applying multiangle analysis. The possibility of the application of this approach in the clear air, outside the smoke plumes, is currently investigated (Kovalev et. al, 2002b).

IV. ACKNOWLEDGEMENTS

This research was supported in part by funds provided by the Rocky Mountain Research Station, Forest Service, U.S. Department of Agriculture. The efforts of Mick

Harrington and the fire crew from the Stevensville Ranger District in conducting the prescribed fire and allowing us to deploy the lidar are greatly appreciated.

V. BIBLIOGRAPHY

Eichinger W., D. Cooper, M. Parlange, and G. Katul. "The Application of a Scanning, Water-Raman Lidar as a Probe of the Atmospheric Boundary Layer", *IEEE Trans. on Geosci. and Remote Sensing,* Vol 31, 1 pp. 70-79, 1993.

Klett, J., "Stable Analytical Inversion Solution for Processing Lidar Returns, "*Appl. Opt.*, **20**, 211-220, 1981.

Kovalev, V., and H. Moosmüller, "Distortion of Particulate Extinction Profiles Measured with Lidar in a Two-component Atmosphere," *Appl. Opt.*, **33**, 6499-6507, 1994.

Kovalev, V., "Sensitivity of the Lidar Equation Solution to Errors in the Aerosol Backscatter-to-extinction Ratio: Influence of a Monotonic Change in the Aerosol Extinction Coefficient," *Appl. Opt.*, **34**, 3457-3462, 1995.

Kovalev, V.A., R.A. Susott, W.E. Eichinger, and Wei Min Hao, Application of a Stable Near-end Solution to Determine the Extinction Coefficient of Smoke Aerosols from Biomass Fires, *Proceedings of the Twenty First International Laser Radar Conference* (Quebec, Canada, 2002), Pt. 1, pp. 247-250, 2002.

Kovalev, V., "Stable Near-end Solution of the Lidar Equation for Clear Atmospheres." (Submitted to Applied Optics, 2002a).

Kovalev, V. A., M. Pahlow, and M. B. Parlange, "Elimination of Asymmetry in the Two-angle Lidar-equation Solution for Aerosol Extinction Profiles ," *Proceedings of the Twenty First International Laser Radar Conference* (Quebec, Canada, 2002), Pt. 2, pp. 621-624, 2002b.

Kunz, G. J., and G. Leeuw (1993), "Inversion of Lidar Signals with the Slope Method," *Appl. Opt.*, **32**, 3249-3256.

Kunz, G. J. (1996), "Transmission as an Input Boundary Value for an Analytical Solution of a Single-scatter Lidar Equation" Appl. Opt., **35**, 3255-3260.

Marenco, F., V. Santacesaria, A. F. Baus, D. Balis, A. di Sarra, A. Papayannis, and C. Zerefos, "Optical Properties of Tropospheric Aerosols Determined by Lidar and Spectrophotometric Measurements (Photochemical Activity and Solar Ultraviolet Radiation Campaign)," *Appl. Opt.*, **36**, 6875-6886, 1997.

Measures, R.M., Laser Remote Sensing, Wiley Interscience, New York, 1984.

Porter J. N., B. Lienert, and S. K. Sharma, "Using horizontal and Slant Lidar Measurements to Obtain Calibrated Aerosol Scattering Coefficients from a Coastal Lidar in Hawaii," *J. Atm. and Ocean Technology*, **17**, 1445-1454.

Rybakov, E. E., V. A. Kovalev, Pak A. S., Mozharov E. E., and G. N., Baldenkov , "Results of the Lidar Determination of Slant Visibility Characteristics at the Airport," *Meteorol. and Hydro.*, **9**, Gidrometeoizdat, Leningrad, U.S.S.R., 18-25, 1991.

Sassen, K., and B. S. Cho, "Subvisual-thin Cirrus Lidar Dataset for Satellite Verification and Climatological Research," *J. Appl. Meteorol.*, **31**, 1275-1285, 1992.

Sicard, M, P. Chazette, J. Pelon, J. G. Won, and S.-C. Yoon , "Variational Method for the Retrievl of the Optical Thickness and the Backscatter Coefficient from Multiangle Lidar Profiles," *Appl. Opt.*, 41, 493-502, 2002.

Weinman, J., "Derivation of Atmospheric Extinction Profiles and Wind Speed over the Ocean from a Satellite-borne Lidar," *Appl. Opt.*, **27**, 3994-4001, 1988.

APPENDIX

Listing of Data Files Taken

All data was taken at 1064 nm except as noted.

07 November 2001

07NOV001.2D, 11/7/2001, 14:38, 676288
Elevation: 20.00 to 60.00 step: 0.50 azimuth: 172.00 shots: 50
Testing for Wind lidar

07NOV002.2D, 11/7/2001, 14:41, 676288
Elevation: 20.00 to 60.00 step: 0.50 azimuth: 172.00 shots: 50
Testing for Wind lidar

07NOV003.2D, 11/7/2001, 14:52, 709552
Elevation: 18.00 to 60.00 step: 0.50 azimuth: 185.00 shots: 50
Vertical Scan over the Fire Line

07NOV004.2D, 11/7/2001, 14:54, 676288
Elevation: 20.00 to 60.00 step: 0.50 azimuth: 172.00 shots: 50
Vertical Scan over the Fire Line

07NOV005.2D, 11/7/2001, 14:58, 676288
Elevation: 20.00 to 60.00 step: 0.50 azimuth: 185.00 shots: 50
Vertical Scan right of the Fire Line

07NOV006.2D, 11/7/2001, 15:1, 709552
Elevation: 18.00 to 60.00 step: 0.50 azimuth: 185.00 shots: 50
Vertical Scan right of the Fire Line

07NOV007.2D, 11/7/2001, 15:3, 726184
Elevation: 17.00 to 60.00 step: 0.50 azimuth: 185.00 shots: 35
Vertical Scan right of the Fire Line

07NOV008.2D, 11/7/2001, 15:5, 726184
Elevation: 17.00 to 60.00 step: 0.50 azimuth: 185.00 shots: 35
Vertical Scan right of the Fire Line

07NOV009.2D, 11/7/2001, 15:6, 726184
Elevation: 17.00 to 60.00 step: 0.50 azimuth: 185.00 shots: 35
Vertical Scan right of the Fire Line

07NOV010.2D, 11/7/2001, 15:9, 726184
Elevation: 17.00 to 60.00 step: 0.50 azimuth: 185.00 shots: 35
Vertical Scan right of the Fire Line

07NOV011.2D, 11/7/2001, 15:10, 742816
Elevation: 16.00 to 60.00 step: 0.50 azimuth: 185.00 shots: 35
Vertical Scan right of the Fire Line

07NOV012.2D, 11/7/2001, 15:12, 742816
Elevation: 16.00 to 60.00 step: 0.50 azimuth: 185.00 shots: 35
Vertical Scan right of the Fire Line

07NOV013.2D, 11/7/2001, 15:14, 742816
Elevation: 16.00 to 60.00 step: 0.50 azimuth: 185.00 shots: 35
Vertical Scan right of the Fire Line

07NOV014.2D, 11/7/2001, 15:15, 742816
Elevation: 16.00 to 60.00 step: 0.50 azimuth: 185.00 shots: 35
Vertical Scan right of the Fire Line

07NOV015.2D, 11/7/2001, 15:17, 742816
Elevation: 16.00 to 60.00 step: 0.50 azimuth: 185.00 shots: 35
Vertical Scan right of the Fire Line

07NOV016.2D, 11/7/2001, 15:20, 676288
Azimuth: 145.00 to 185.00 step: 0.50 Elevation: 20.00 shots: 35
Vertical Scan right of the Fire Line

07NOV017.2D, 11/7/2001, 15:22, 676288
Azimuth: 145.00 to 185.00 step: 0.50 Elevation: 18.00 shots: 35
Vertical Scan right of the Fire Line

07NOV018.2D, 11/7/2001, 15:29, 676288
Azimuth: 145.00 to 185.00 step: 0.50 Elevation: 18.00 shots: 35
Vertical Scan right of the Fire Line

07NOV019.2D, 11/7/2001, 15:30, 676288
Azimuth: 145.00 to 185.00 step: 0.50 Elevation: 18.00 shots: 35
Vertical Scan right of the Fire Line

07NOV020.2D, 11/7/2001, 15:32, 676288
Azimuth: 145.00 to 185.00 step: 0.50 Elevation: 20.00 shots: 35
Vertical Scan right of the Fire Line

07NOV021.2D, 11/7/2001, 15:34, 676288
Azimuth: 145.00 to 185.00 step: 0.50 Elevation: 20.00 shots: 35
Vertical Scan right of the Fire Line

07NOV022.2D, 11/7/2001, 15:36, 692920
Azimuth: 145.00 to 186.00 step: 0.50 Elevation: 20.00 shots: 35
Vertical Scan right of the Fire Line

07NOV023.2D, 11/7/2001, 15:37, 692920
Azimuth: 145.00 to 186.00 step: 0.50 Elevation: 20.00 shots: 35
Vertical Scan right of the Fire Line

07NOV024.2D, 11/7/2001, 15:38, 692920
Azimuth: 145.00 to 186.00 step: 0.50 Elevation: 20.00 shots: 35
Vertical Scan right of the Fire Line

07NOV025.2D, 11/7/2001, 15:40, 692920
Azimuth: 145.00 to 186.00 step: 0.50 Elevation: 20.00 shots: 35
Vertical Scan right of the Fire Line

07NOV026.2D, 11/7/2001, 15:42, 692920
Azimuth: 145.00 to 186.00 step: 0.50 Elevation: 20.00 shots: 35
Vertical Scan right of the Fire Line

07NOV027.COR, 11/7/2001, 15:49, 2497492
Azimuth: 175.00 step: 2.50Elevation: 20.00 step: 0.00 shots: 20
Vertical Scan right of the Fire Line

07NOV028.COR, 11/7/2001, 15:55, 2497492
Azimuth: 175.00 step: 0.00Elevation: 24.00 step: 3.00 shots: 20
Vertical Scan right of the Fire Line

07NOV029.COR, 11/7/2001, 16:0, 2497492
Azimuth: 175.00 step: 0.00Elevation: 21.00 step: 1.00 shots: 20
Vertical Scan right of the Fire Line

07NOV030.2D, 11/7/2001, 16:3, 759448
Elevation: 0.00 to 45.00 step: 0.50 azimuth: 63.00 shots: 50
Vertical Scan right of the Fire Line

07NOV031.2D, 11/7/2001, 16:6, 759448
Elevation: 0.00 to 45.00 step: 0.50 azimuth: 63.00 shots: 50
Down the Valley

07NOV032.2D, 11/7/2001, 16:8, 759448
Elevation: 0.00 to 45.00 step: 0.50 azimuth: 63.00 shots: 50
Down the Valley
07NOV033.2D, 11/7/2001, 16:11, 385228
Elevation: 0.00 to 45.00 step: 1.00 azimuth: 63.00 shots: 100
Down the Valley
07NOV034.2D, 11/7/2001, 16:14, 385228
Elevation: 0.00 to 45.00 step: 1.00 azimuth: 63.00 shots: 100
Down the Valley
07NOV035.2D, 11/7/2001, 16:16, 385228
Elevation: 0.00 to 45.00 step: 1.00 azimuth: 63.00 shots: 100
Down the Valley
07NOV036.2D, 11/7/2001, 16:18, 401860
Elevation: -2.00 to 45.00 step: 1.00 azimuth: 63.00 shots: 100
Down the Valley
07NOV037.COR, 11/7/2001, 16:30, 2497492
Azimuth: 175.00 step: 2.00Elevation: 19.00 step: 0.00 shots: 20
Correlation of the Fire Line
07NOV038.2D, 11/7/2001, 16:31, 692920
Azimuth: 145.00 to 186.00 step: 0.50 Elevation: 20.00 shots: 50
Vertical Scan over the Fire Line
07NOV039.DAT, 11/7/2001, 16:35, 10884
Azimuth: 145.00 Elevation: 20.00 shots: 50
Vertical Scan over the Fire Line
07NOV039.2D, 11/7/2001, 16:32, 2692
Elevation: 18.00 to 60.00 step: 0.50 azimuth: 185.00 shots: 50
Vertical Scan over the Fire Line
07NOV040.2D, 11/7/2001, 16:35, 692920
Azimuth: 145.00 to 186.00 step: 0.50 Elevation: 20.00 shots: 50
Vertical Scan over the Fire Line
07NOV041.2D, 11/7/2001, 16:37, 709552
Elevation: 18.00 to 60.00 step: 0.50 azimuth: 185.00 shots: 50
Vertical Scan over the Fire Line
07NOV042.2D, 11/7/2001, 16:39, 709552
Elevation: 18.00 to 60.00 step: 0.50 azimuth: 185.00 shots: 50
Vertical Scan over the Fire Line
07NOV043.2D, 11/7/2001, 16:41, 676288
Elevation: 20.00 to 60.00 step: 0.50 azimuth: 172.00 shots: 50
Vertical Scan over the Fire Line
07NOV044.2D, 11/7/2001, 16:43, 709552
Elevation: 18.00 to 60.00 step: 0.50 azimuth: 155.00 shots: 50
Vertical Scan left of the Fire Line
07NOV045.COR, 11/7/2001, 16:48, 2497492
Azimuth: 175.00 step: 0.00Elevation: 19.00 step: 1.00 shots: 20
Correlation of the Fire Line
07NOV046.COR, 11/7/2001, 16:53, 2497492
Azimuth: 175.00 step: 0.00Elevation: 20.00 step: 2.00 shots: 20
Correlation of the Fire Line
07NOV047.COR, 11/7/2001, 16:58, 2497492
Azimuth: 175.00 step: 1.00Elevation: 19.00 step: 0.00 shots: 20
Correlation of the Fire Line
07NOV048.COR, 11/7/2001, 17:3, 2497492
Azimuth: 175.00 step: 2.00Elevation: 19.00 step: 0.00 shots: 20
Correlation of the Fire Line
07NOV049.2D, 11/7/2001, 17:3, 692920
Azimuth: 145.00 to 186.00 step: 0.50 Elevation: 20.00 shots: 50
Vertical Scan over the Fire Line
07NOV050.2D, 11/7/2001, 17:5, 709552
Elevation: 18.00 to 60.00 step: 0.50 azimuth: 185.00 shots: 50
Vertical Scan over the Fire Line
07NOV051.2D, 11/7/2001, 17:7, 709552
Elevation: 18.00 to 60.00 step: 0.50 azimuth: 185.00 shots: 50
Vertical Scan over the Fire Line
07NOV052.2D, 11/7/2001, 17:9, 676288
Elevation: 20.00 to 60.00 step: 0.50 azimuth: 172.00 shots: 50
Vertical Scan over the Fire Line
07NOV053.2D, 11/7/2001, 17:11, 110800
Elevation: 18.00 to 60.00 step: 0.50 azimuth: 155.00 shots: 50
Vertical Scan left of the Fire Line

08 November 2001

08NOV001.2D, 11/8/2001, 14:38, 401860
Elevation: 12.66 to 60.00 step: 1.00 azimuth: 94.40 shots: 50
Missoula Fire Experiment
08NOV002.2D, 11/8/2001, 14:41, 401860
Elevation: 13.00 to 60.00 step: 1.00 azimuth: 113.00 shots: 50
Missoula Fire Experiment
08NOV003.2D, 11/8/2001, 14:44, 742816
Elevation: 16.00 to 60.00 step: 0.50 azimuth: 113.00 shots: 50
Missoula Fire Experiment
08NOV004.2D, 11/8/2001, 14:46, 742816
Elevation: 16.00 to 60.00 step: 0.50 azimuth: 113.00 shots: 50
Missoula Fire Experiment
08NOV005.2D, 11/8/2001, 14:49, 742816
Elevation: 16.00 to 60.00 step: 0.50 azimuth: 113.00 shots: 50
Missoula Fire Experiment
08NOV006.2D, 11/8/2001, 14:52, 2692
Elevation: 16.00 to 60.00 step: 0.50 azimuth: 108.00 shots: 50
Missoula Fire Experiment
08NOV006.DAT, 11/8/2001, 15:2, 10884
Azimuth: 108.00 Elevation: 41.56 shots: 50
Missoula Fire Experiment
08NOV007.DAT, 11/8/2001, 15:2, 10884
Azimuth: 108.00 Elevation: 41.56 shots: 100
Missoula Fire Experiment
08NOV008.DAT, 11/8/2001, 15:8, 10884
Azimuth: 108.00 Elevation: 41.56 shots: 100
Missoula Fire Experiment
08NOV009.DAT, 11/8/2001, 15:9, 10884
Azimuth: 108.00 Elevation: 41.56 shots: 500
Missoula Fire Experiment

08NOV011.2D, 11/8/2001, 15:17, 559864
Azimuth: 95.00 to 128.00 step: 0.50 Elevation: 17.00 shots: 50
Missoula Fire Experiment
08NOV012.2D, 11/8/2001, 15:19, 726184
Azimuth: 95.00 to 138.00 step: 0.50 Elevation: 17.00 shots: 50
Missoula Fire Experiment
08NOV013.2D, 11/8/2001, 15:21, 759448
Azimuth: 100.00 to 145.00 step: 0.50 Elevation: 19.00 shots: 50
Missoula Fire Experiment
08NOV014.2D, 11/8/2001, 15:24, 343648
Azimuth: 100.00 to 140.00 step: 1.00 Elevation: 19.00 shots: 10
Missoula Fire Experiment
08NOV015.2D, 11/8/2001, 15:24, 343648
Azimuth: 100.00 to 140.00 step: 1.00 Elevation: 19.00 shots: 10
Missoula Fire Experiment
08NOV016.2D, 11/8/2001, 15:25, 343648
Azimuth: 100.00 to 140.00 step: 1.00 Elevation: 19.00 shots: 10
Missoula Fire Experiment
08NOV017.2D, 11/8/2001, 15:26, 218908
Azimuth: 105.00 to 136.00 step: 1.25 Elevation: 19.00 shots: 5
Missoula Fire Experiment
08NOV018.2D, 11/8/2001, 15:26, 218908
Azimuth: 105.00 to 136.00 step: 1.25 Elevation: 19.00 shots: 5
Missoula Fire Experiment
08NOV019.2D, 11/8/2001, 15:27, 218908
Azimuth: 105.00 to 136.00 step: 1.25 Elevation: 19.00 shots: 5
Missoula Fire Experiment
08NOV020.2D, 11/8/2001, 15:27, 218908
Azimuth: 105.00 to 136.00 step: 1.25 Elevation: 19.00 shots: 5
Missoula Fire Experiment
08NOV021.2D, 11/8/2001, 15:27, 218908
Azimuth: 105.00 to 136.00 step: 1.25 Elevation: 19.00 shots: 5
Missoula Fire Experiment
08NOV022.2D, 11/8/2001, 15:28, 218908
Azimuth: 105.00 to 136.00 step: 1.25 Elevation: 19.00 shots: 5
Missoula Fire Experiment
08NOV023.2D, 11/8/2001, 15:28, 218908
Azimuth: 105.00 to 136.00 step: 1.25 Elevation: 19.00 shots: 5
Missoula Fire Experiment
08NOV024.2D, 11/8/2001, 15:28, 218908
Azimuth: 105.00 to 136.00 step: 1.25 Elevation: 19.00 shots: 5
Missoula Fire Experiment
08NOV025.2D, 11/8/2001, 15:29, 218908
Azimuth: 105.00 to 136.00 step: 1.25 Elevation: 19.00 shots: 5
Missoula Fire Experiment
08NOV026.TD, 11/8/2001, 15:30, 4160692
Azimuth: 116.00 Elevation: 19.00 shots: 10
Missoula Fire Experiment
08NOV027.TD, 11/8/2001, 15:33, 6239692
Azimuth: 116.00 Elevation: 19.00 shots: 10
Missoula Fire Experiment
08NOV028.TD, 11/8/2001, 15:36, 6239692
Azimuth: 116.00 Elevation: 19.00 shots: 10
Missoula Fire Experiment
08NOV029.TD, 11/8/2001, 15:39, 6239692
Azimuth: 116.00 Elevation: 19.00 shots: 10
Missoula Fire Experiment
08NOV030.TD, 11/8/2001, 15:49, 6239692
Azimuth: 116.00 Elevation: 17.99 shots: 10
Missoula Fire Experiment
08NOV031.TD, 11/8/2001, 15:52, 6239692
Azimuth: 116.00 Elevation: 19.00 shots: 10
Missoula Fire Experiment
08NOV032.TD, 11/8/2001, 15:55, 6239692
Azimuth: 116.00 Elevation: 19.00 shots: 10
Missoula Fire Experiment
08NOV033.TD, 11/8/2001, 15:58, 6239692
Azimuth: 116.00 Elevation: 19.00 shots: 10
Missoula Fire Experiment

Files numbered 08Nov034 through 09Nov042 were made at 532 nm

08NOV034.2D, 11/8/2001, 16:6, 1058824
Elevation: -3.00 to 60.00 step: 0.50 azimuth: 4.50 shots: 50
Missoula Fire Experiment
08NOV035.2D, 11/8/2001, 16:10, 1058824
Elevation: -3.00 to 60.00 step: 0.50 azimuth: 4.50 shots: 50
Missoula Fire Experiment
08NOV036.2D, 11/8/2001, 16:14, 809344
Elevation: -3.00 to 45.00 step: 0.50 azimuth: 4.50 shots: 50
Missoula Fire Experiment
08NOV037.2D, 11/8/2001, 16:17, 809344
Elevation: -3.00 to 45.00 step: 0.50 azimuth: 4.50 shots: 50
Missoula Fire Experiment
08NOV038.DAT, 11/8/2001, 16:23, 10884
Azimuth: 4.50 Elevation: 0.00 shots: 1000
Missoula Fire Experiment
08NOV039.DAT, 11/8/2001, 16:23, 10884
Azimuth: 4.50 Elevation: 0.00 shots: 1000
Missoula Fire Experiment
08NOV040.DAT, 11/8/2001, 16:24, 10884
Azimuth: 4.50 Elevation: 0.00 shots: 1000
Missoula Fire Experiment
08NOV041.2D, 11/8/2001, 16:26, 809344
Elevation: -3.00 to 45.00 step: 0.50 azimuth: 4.50 shots: 50
Missoula Fire Experiment
08NOV042.2D, 11/8/2001, 16:33, 2692
Elevation: -3.00 to 45.00 step: 0.50 azimuth: 4.50 shots: 50
Missoula Fire Experiment
08NOV042.DAT, 11/8/2001, 16:37, 10884

Azimuth: 4.50 Elevation: 0.00 shots: 1000
Missoula Fire Experiment

Files numbered 08Nov034 through 09Nov042 were made at 532 nm

08NOV043.DAT, 11/8/2001, 16:38, 10884
Azimuth: 4.50 Elevation: 0.00 shots: 1000
Missoula Fire Experiment
08NOV044.DAT, 11/8/2001, 16:38, 10884
Azimuth: 4.50 Elevation: 0.00 shots: 1000
Missoula Fire Experiment
08NOV045.2D, 11/8/2001, 16:40, 809344
Elevation: -3.00 to 45.00 step: 0.50 azimuth: 4.50 shots: 50
Missoula Fire Experiment
08NOV046.2D, 11/8/2001, 16:42, 809344
Elevation: -3.00 to 45.00 step: 0.50 azimuth: 4.50 shots: 50
Missoula Fire Experiment
08NOV047.2D, 11/8/2001, 16:45, 809344
Elevation: -3.00 to 45.00 step: 0.50 azimuth: 4.50 shots: 50
Missoula Fire Experiment
08NOV048.2D, 11/8/2001, 16:47, 809344
Elevation: -3.00 to 45.00 step: 0.50 azimuth: 4.50 shots: 50
Missoula Fire Experiment
08NOV049.DAT, 11/8/2001, 16:53, 10884
Azimuth: 4.50 Elevation: 86.00 shots: 500
Missoula Fire Experiment
08NOV050.DAT, 11/8/2001, 16:54, 10884
Azimuth: 4.50 Elevation: 86.00 shots: 500
Missoula Fire Experiment
08NOV051.DAT, 11/8/2001, 16:54, 10884
Azimuth: 4.50 Elevation: 86.00 shots: 500
Missoula Fire Experiment

09 November 2001

09NOV001.DAT, 11/9/2001, 14:26, 10884
Azimuth: 92.80 Elevation: 12.46 shots: 50
Missoula Fire Experiment
09NOV001.TD, 11/9/2001, 14:25, 734500
Azimuth: 92.80 Elevation: 12.46 shots: 50
Missoula Fire Experiment
09NOV002.TD, 11/9/2001, 14:27, 4160692
Azimuth: 92.80 Elevation: 12.46 shots: 20
Missoula Fire Experiment
09NOV003.TD, 11/9/2001, 14:31, 8318692
Azimuth: 92.80 Elevation: 12.46 shots: 10
Missoula Fire Experiment
09NOV004.2D, 11/9/2001, 14:41, 1507888
Azimuth: 50.00 to 140.00 step: 0.50 Elevation: 17.46 shots: 50
Missoula Fire Experiment
09NOV005.2D, 11/9/2001, 14:48, 1507888
Azimuth: 50.00 to 140.00 step: 0.50 Elevation: 16.00 shots: 20
Missoula Fire Experiment
09NOV006.2D, 11/9/2001, 14:50, 1507888
Azimuth: 50.00 to 140.00 step: 0.50 Elevation: 16.00 shots: 20
Missoula Fire Experiment
09NOV007.3D, 11/9/2001, 14:55, 7162768
Elevation: 8.00 to 18.00 step: 0.50 azimuth: 65.00 to 85.00
step: 0.50 shots: 10
Missoula Fire Experiment

Files numbered 09Nov008 through 09Nov075 were made at 532 nm

09NOV008.3D, 11/9/2001, 15:4, 2564020
Elevation: 8.00 to 18.00 step: 1.00 azimuth: 65.00 to 85.00
step: 0.75 shots: 5
Missoula Fire Experiment
09NOV009.2D, 11/9/2001, 15:9, 626392
Elevation: 8.00 to 45.00 step: 0.50 azimuth: 70.00 shots: 10
Missoula Fire Experiment
09NOV010.2D, 11/9/2001, 15:10, 293752
Elevation: 8.00 to 25.00 step: 0.50 azimuth: 70.00 shots: 10
Missoula Fire Experiment
09NOV011.2D, 11/9/2001, 15:10, 293752
Elevation: 8.00 to 25.00 step: 0.50 azimuth: 70.00 shots: 10
Missoula Fire Experiment
09NOV012.2D, 11/9/2001, 15:11, 293752
Elevation: 8.00 to 25.00 step: 0.50 azimuth: 70.00 shots: 10
Missoula Fire Experiment
09NOV013.2D, 11/9/2001, 15:11, 293752
Elevation: 8.00 to 25.00 step: 0.50 azimuth: 70.00 shots: 10
Missoula Fire Experiment
09NOV014.2D, 11/9/2001, 15:11, 293752
Elevation: 8.00 to 25.00 step: 0.50 azimuth: 70.00 shots: 10
Missoula Fire Experiment
09NOV015.2D, 11/9/2001, 15:12, 293752
Elevation: 8.00 to 25.00 step: 0.50 azimuth: 70.00 shots: 10
Missoula Fire Experiment
09NOV016.2D, 11/9/2001, 15:12, 293752
Elevation: 8.00 to 25.00 step: 0.50 azimuth: 70.00 shots: 10
Missoula Fire Experiment
09NOV017.2D, 11/9/2001, 15:12, 293752
Elevation: 8.00 to 25.00 step: 0.50 azimuth: 70.00 shots: 10
Missoula Fire Experiment
09NOV018.2D, 11/9/2001, 15:13, 293752
Elevation: 8.00 to 25.00 step: 0.50 azimuth: 70.00 shots: 10
Missoula Fire Experiment
09NOV019.2D, 11/9/2001, 15:13, 293752
Elevation: 8.00 to 25.00 step: 0.50 azimuth: 70.00 shots: 10
Missoula Fire Experiment
09NOV020.2D, 11/9/2001, 15:13, 293752
Elevation: 8.00 to 25.00 step: 0.50 azimuth: 70.00 shots: 10
Missoula Fire Experiment
09NOV021.2D, 11/9/2001, 15:14, 293752

Elevation: 8.00 to 25.00 step: 0.50 azimuth: 70.00 shots: 10
Missoula Fire Experiment
09NOV022.2D, 11/9/2001, 15:14, 293752
Elevation: 8.00 to 25.00 step: 0.50 azimuth: 70.00 shots: 10
Missoula Fire Experiment
09NOV023.2D, 11/9/2001, 15:14, 293752
Elevation: 8.00 to 25.00 step: 0.50 azimuth: 70.00 shots: 10
Missoula Fire Experiment
09NOV024.2D, 11/9/2001, 15:15, 293752
Elevation: 8.00 to 25.00 step: 0.50 azimuth: 70.00 shots: 10
Missoula Fire Experiment
09NOV025.2D, 11/9/2001, 15:15, 293752
Elevation: 8.00 to 25.00 step: 0.50 azimuth: 70.00 shots: 10
Missoula Fire Experiment
09NOV026.2D, 11/9/2001, 15:15, 293752
Elevation: 8.00 to 25.00 step: 0.50 azimuth: 70.00 shots: 10
Missoula Fire Experiment
09NOV027.2D, 11/9/2001, 15:15, 293752
Elevation: 8.00 to 25.00 step: 0.50 azimuth: 70.00 shots: 10
Missoula Fire Experiment
09NOV028.2D, 11/9/2001, 15:16, 293752
Elevation: 8.00 to 25.00 step: 0.50 azimuth: 70.00 shots: 10
Missoula Fire Experiment
09NOV029.2D, 11/9/2001, 15:16, 293752
Elevation: 8.00 to 25.00 step: 0.50 azimuth: 70.00 shots: 10
Missoula Fire Experiment
09NOV030.2D, 11/9/2001, 15:16, 293752
Elevation: 8.00 to 25.00 step: 0.50 azimuth: 70.00 shots: 10
Missoula Fire Experiment
09NOV031.2D, 11/9/2001, 15:18, 293752
Elevation: 8.00 to 25.00 step: 0.50 azimuth: 70.00 shots: 5
Missoula Fire Experiment
09NOV032.2D, 11/9/2001, 15:18, 293752
Elevation: 8.00 to 25.00 step: 0.50 azimuth: 70.00 shots: 5
Missoula Fire Experiment
09NOV033.2D, 11/9/2001, 15:19, 293752
Elevation: 8.00 to 25.00 step: 0.50 azimuth: 70.00 shots: 5
Missoula Fire Experiment
09NOV034.2D, 11/9/2001, 15:19, 293752
Elevation: 8.00 to 25.00 step: 0.50 azimuth: 70.00 shots: 5
Missoula Fire Experiment
09NOV035.2D, 11/9/2001, 15:19, 293752
Elevation: 8.00 to 25.00 step: 0.50 azimuth: 70.00 shots: 5
Missoula Fire Experiment
09NOV036.2D, 11/9/2001, 15:19, 293752
Elevation: 8.00 to 25.00 step: 0.50 azimuth: 70.00 shots: 5
Missoula Fire Experiment
09NOV037.2D, 11/9/2001, 15:20, 293752
Elevation: 8.00 to 25.00 step: 0.50 azimuth: 70.00 shots: 5
Missoula Fire Experiment
09NOV038.2D, 11/9/2001, 15:20, 293752
Elevation: 8.00 to 25.00 step: 0.50 azimuth: 70.00 shots: 5
Missoula Fire Experiment
09NOV039.2D, 11/9/2001, 15:20, 293752
Elevation: 8.00 to 25.00 step: 0.50 azimuth: 70.00 shots: 5
Missoula Fire Experiment
09NOV040.2D, 11/9/2001, 15:20, 293752
Elevation: 8.00 to 25.00 step: 0.50 azimuth: 70.00 shots: 5
Missoula Fire Experiment
09NOV041.2D, 11/9/2001, 15:21, 293752
Elevation: 8.00 to 25.00 step: 0.50 azimuth: 70.00 shots: 5
Missoula Fire Experiment
09NOV042.2D, 11/9/2001, 15:21, 293752
Elevation: 8.00 to 25.00 step: 0.50 azimuth: 70.00 shots: 5
Missoula Fire Experiment
09NOV043.2D, 11/9/2001, 15:21, 293752
Elevation: 8.00 to 25.00 step: 0.50 azimuth: 70.00 shots: 5
Missoula Fire Experiment
09NOV044.2D, 11/9/2001, 15:21, 293752
Elevation: 8.00 to 25.00 step: 0.50 azimuth: 70.00 shots: 5
Missoula Fire Experiment
09NOV045.2D, 11/9/2001, 15:22, 293752
Elevation: 8.00 to 25.00 step: 0.50 azimuth: 70.00 shots: 5
Missoula Fire Experiment
09NOV046.2D, 11/9/2001, 15:22, 293752
Elevation: 8.00 to 25.00 step: 0.50 azimuth: 70.00 shots: 5
Missoula Fire Experiment
09NOV047.2D, 11/9/2001, 15:22, 293752
Elevation: 8.00 to 25.00 step: 0.50 azimuth: 70.00 shots: 5
Missoula Fire Experiment
09NOV048.2D, 11/9/2001, 15:22, 293752
Elevation: 8.00 to 25.00 step: 0.50 azimuth: 70.00 shots: 5
Missoula Fire Experiment
09NOV049.2D, 11/9/2001, 15:23, 293752
Elevation: 8.00 to 25.00 step: 0.50 azimuth: 70.00 shots: 5
Missoula Fire Experiment
09NOV050.2D, 11/9/2001, 15:23, 293752
Elevation: 8.00 to 25.00 step: 0.50 azimuth: 70.00 shots: 5
Missoula Fire Experiment
09NOV051.2D, 11/9/2001, 15:23, 293752
Elevation: 8.00 to 25.00 step: 0.50 azimuth: 70.00 shots: 5
Missoula Fire Experiment
09NOV052.2D, 11/9/2001, 15:25, 293752
Elevation: 8.00 to 25.00 step: 0.50 azimuth: 70.00 shots: 2
Missoula Fire Experiment
09NOV053.2D, 11/9/2001, 15:25, 293752
Elevation: 8.00 to 25.00 step: 0.50 azimuth: 70.00 shots: 2
Missoula Fire Experiment
09NOV054.2D, 11/9/2001, 15:25, 293752
Elevation: 8.00 to 25.00 step: 0.50 azimuth: 70.00 shots: 2
Missoula Fire Experiment
09NOV055.2D, 11/9/2001, 15:25, 293752
Elevation: 8.00 to 25.00 step: 0.50 azimuth: 70.00 shots: 2
Missoula Fire Experiment

09NOV056.2D, 11/9/2001, 15:25, 293752
Elevation: 8.00 to 25.00 step: 0.50 azimuth: 70.00 shots: 2
Missoula Fire Experiment
09NOV057.2D, 11/9/2001, 15:26, 293752
Elevation: 8.00 to 25.00 step: 0.50 azimuth: 70.00 shots: 2
Missoula Fire Experiment
09NOV058.2D, 11/9/2001, 15:26, 293752
Elevation: 8.00 to 25.00 step: 0.50 azimuth: 70.00 shots: 2
Missoula Fire Experiment
09NOV059.2D, 11/9/2001, 15:26, 293752
Elevation: 8.00 to 25.00 step: 0.50 azimuth: 70.00 shots: 2
Missoula Fire Experiment
09NOV060.2D, 11/9/2001, 15:26, 293752
Elevation: 8.00 to 25.00 step: 0.50 azimuth: 70.00 shots: 2
Missoula Fire Experiment
09NOV061.2D, 11/9/2001, 15:27, 293752
Elevation: 8.00 to 25.00 step: 0.50 azimuth: 70.00 shots: 2
Missoula Fire Experiment
09NOV062.2D, 11/9/2001, 15:27, 293752
Elevation: 8.00 to 25.00 step: 0.50 azimuth: 70.00 shots: 2
Missoula Fire Experiment
09NOV063.2D, 11/9/2001, 15:27, 293752
Elevation: 8.00 to 25.00 step: 0.50 azimuth: 70.00 shots: 2
Missoula Fire Experiment
09NOV064.2D, 11/9/2001, 15:27, 293752
Elevation: 8.00 to 25.00 step: 0.50 azimuth: 70.00 shots: 2
Missoula Fire Experiment
09NOV065.2D, 11/9/2001, 15:27, 293752
Elevation: 8.00 to 25.00 step: 0.50 azimuth: 70.00 shots: 2
Missoula Fire Experiment
09NOV066.2D, 11/9/2001, 15:28, 293752
Elevation: 8.00 to 25.00 step: 0.50 azimuth: 70.00 shots: 2
Missoula Fire Experiment
09NOV067.2D, 11/9/2001, 15:28, 293752
Elevation: 8.00 to 25.00 step: 0.50 azimuth: 70.00 shots: 2
Missoula Fire Experiment
09NOV068.2D, 11/9/2001, 15:28, 293752
Elevation: 8.00 to 25.00 step: 0.50 azimuth: 70.00 shots: 2
Missoula Fire Experiment
09NOV069.2D, 11/9/2001, 15:28, 293752
Elevation: 8.00 to 25.00 step: 0.50 azimuth: 70.00 shots: 2
Missoula Fire Experiment
09NOV070.2D, 11/9/2001, 15:29, 293752
Elevation: 8.00 to 25.00 step: 0.50 azimuth: 70.00 shots: 2
Missoula Fire Experiment
09NOV071.2D, 11/9/2001, 15:29, 293752
Elevation: 8.00 to 25.00 step: 0.50 azimuth: 70.00 shots: 2
Missoula Fire Experiment
09NOV072.2D, 11/9/2001, 15:32, 1025560
Azimuth: 35.00 to 96.00 step: 0.50 Elevation: 9.00 shots: 10
Missoula Fire Experiment
09NOV073.2D, 11/9/2001, 15:34, 1025560
Azimuth: 35.00 to 96.00 step: 0.50 Elevation: 9.00 shots: 10
Missoula Fire Experiment
09NOV074.2D, 11/9/2001, 15:35, 1025560
Azimuth: 35.00 to 96.00 step: 0.50 Elevation: 9.00 shots: 10
Missoula Fire Experiment
09NOV075.2D, 11/9/2001, 15:36, 1025560
Azimuth: 35.00 to 96.00 step: 0.50 Elevation: 9.00 shots: 50
Missoula Fire Experiment

Files numbered 09Nov008 through 09Nov075 were made at 532 nm

09NOV076.DAT, 11/9/2001, 15:48, 10884
Azimuth: 45.48 Elevation: 3.99 shots: 500
noise
09NOV077.DAT, 11/9/2001, 15:48, 10884
Azimuth: 45.48 Elevation: 3.99 shots: 500
noise
09NOV078.2D, 11/9/2001, 15:53, 634708
Elevation: 7.50 to 45.00 step: 0.50 azimuth: 66.78 shots: 10
experiment
09NOV079.2D, 11/9/2001, 15:54, 634708
Elevation: 7.50 to 45.00 step: 0.50 azimuth: 66.78 shots: 10
experiment
09NOV080.2D, 11/9/2001, 15:58, 559864
Azimuth: 62.00 to 95.00 step: 0.50 Elevation: 9.00 shots: 10
experiment
09NOV081.2D, 11/9/2001, 15:58, 559864
Azimuth: 62.00 to 95.00 step: 0.50 Elevation: 9.00 shots: 10
experiment
09NOV082.2D, 11/9/2001, 15:59, 559864
Azimuth: 62.00 to 95.00 step: 0.50 Elevation: 9.00 shots: 10
experiment
09NOV083.2D, 11/9/2001, 16:0, 559864
Azimuth: 62.00 to 95.00 step: 0.50 Elevation: 9.00 shots: 50
experiment
09NOV084.2D, 11/9/2001, 16:1, 559864
Azimuth: 62.00 to 95.00 step: 0.50 Elevation: 9.00 shots: 50
experiment
09NOV085.2D, 11/9/2001, 16:16, 759448
Azimuth: 50.00 to 95.00 step: 0.50 Elevation: 8.00 shots: 20
Missoula Fire Experiment
09NOV086.2D, 11/9/2001, 16:17, 759448
Azimuth: 50.00 to 95.00 step: 0.50 Elevation: 8.00 shots: 20
Missoula Fire Experiment
09NOV087.2D, 11/9/2001, 16:20, 759448
Azimuth: 50.00 to 95.00 step: 0.50 Elevation: 8.00 shots: 20
Missoula Fire Experiment
09NOV088.2D, 11/9/2001, 16:22, 1175248
Azimuth: 95.00 to 165.00 step: 0.50 Elevation: 16.00 shots: 20
Missoula Fire Experiment
09NOV089.2D, 11/9/2001, 16:24, 842608
Azimuth: 95.00 to 145.00 step: 0.50 Elevation: 16.00 shots: 20

Missoula Fire Experiment
09NOV090.2D, 11/9/2001, 16:25, 842608
Azimuth: 95.00 to 145.00 step: 0.50 Elevation: 16.00 shots: 20
Missoula Fire Experiment
09NOV091.2D, 11/9/2001, 16:27, 842608
Azimuth: 95.00 to 145.00 step: 0.50 Elevation: 16.00 shots: 35
Missoula Fire Experiment
09NOV092.2D, 11/9/2001, 16:29, 1175248
Azimuth: 75.00 to 145.00 step: 0.50 Elevation: 16.00 shots: 35
Missoula Fire Experiment
09NOV093.2D, 11/9/2001, 16:32, 1341568
Azimuth: 65.00 to 145.00 step: 0.50 Elevation: 16.00 shots: 35
Missoula Fire Experiment
09NOV094.2D, 11/9/2001, 16:36, 177328
Azimuth: 125.00 to 135.00 step: 0.50 Elevation: 16.00 shots: 5
Missoula Fire Experiment
09NOV095.2D, 11/9/2001, 16:37, 177328
Azimuth: 125.00 to 135.00 step: 0.50 Elevation: 16.00 shots: 5
Missoula Fire Experiment
09NOV096.2D, 11/9/2001, 16:37, 177328
Azimuth: 125.00 to 135.00 step: 0.50 Elevation: 16.00 shots: 5
Missoula Fire Experiment
09NOV097.2D, 11/9/2001, 16:38, 177328
Azimuth: 125.00 to 135.00 step: 0.50 Elevation: 16.00 shots: 5
Missoula Fire Experiment
09NOV098.2D, 11/9/2001, 16:38, 177328
Azimuth: 125.00 to 135.00 step: 0.50 Elevation: 16.00 shots: 5
Missoula Fire Experiment
09NOV099.2D, 11/9/2001, 16:38, 85852
Azimuth: 125.00 to 135.00 step: 0.50 Elevation: 16.00 shots: 5
Missoula Fire Experiment
09NOV100.2D, 11/9/2001, 16:39, 343648
Azimuth: 120.00 to 140.00 step: 0.50 Elevation: 16.00 shots: 5
Missoula Fire Experiment
09NOV101.2D, 11/9/2001, 16:39, 343648
Azimuth: 120.00 to 140.00 step: 0.50 Elevation: 16.00 shots: 5
Missoula Fire Experiment
09NOV102.2D, 11/9/2001, 16:39, 343648
Azimuth: 120.00 to 140.00 step: 0.50 Elevation: 16.00 shots: 5
Missoula Fire Experiment
09NOV103.2D, 11/9/2001, 16:39, 343648
Azimuth: 120.00 to 140.00 step: 0.50 Elevation: 16.00 shots: 5
Missoula Fire Experiment
09NOV104.2D, 11/9/2001, 16:40, 343648
Azimuth: 120.00 to 140.00 step: 0.50 Elevation: 16.00 shots: 5
Missoula Fire Experiment
09NOV105.2D, 11/9/2001, 16:40, 343648
Azimuth: 120.00 to 140.00 step: 0.50 Elevation: 16.00 shots: 5
Missoula Fire Experiment
09NOV106.2D, 11/9/2001, 16:40, 343648
Azimuth: 120.00 to 140.00 step: 0.50 Elevation: 16.00 shots: 5
Missoula Fire Experiment
09NOV107.2D, 11/9/2001, 16:41, 343648
Azimuth: 120.00 to 140.00 step: 0.50 Elevation: 16.00 shots: 5
Missoula Fire Experiment
09NOV108.2D, 11/9/2001, 16:41, 343648
Azimuth: 120.00 to 140.00 step: 0.50 Elevation: 16.00 shots: 5
Missoula Fire Experiment
09NOV109.2D, 11/9/2001, 16:41, 343648
Azimuth: 120.00 to 140.00 step: 0.50 Elevation: 16.00 shots: 5
Missoula Fire Experiment
09NOV110.2D, 11/9/2001, 16:41, 77536
Azimuth: 120.00 to 140.00 step: 0.50 Elevation: 16.00 shots: 5
Missoula Fire Experiment
09NOV111.2D, 11/9/2001, 16:42, 260488
Azimuth: 110.00 to 140.00 step: 1.00 Elevation: 16.00 shots: 3
Missoula Fire Experiment
09NOV112.2D, 11/9/2001, 16:43, 260488
Azimuth: 110.00 to 140.00 step: 1.00 Elevation: 16.00 shots: 3
Missoula Fire Experiment
09NOV113.2D, 11/9/2001, 16:43, 260488
Azimuth: 110.00 to 140.00 step: 1.00 Elevation: 16.00 shots: 3
Missoula Fire Experiment
09NOV114.2D, 11/9/2001, 16:43, 260488
Azimuth: 110.00 to 140.00 step: 1.00 Elevation: 16.00 shots: 3
Missoula Fire Experiment
09NOV115.2D, 11/9/2001, 16:43, 260488
Azimuth: 110.00 to 140.00 step: 1.00 Elevation: 16.00 shots: 3
Missoula Fire Experiment
09NOV116.2D, 11/9/2001, 16:44, 260488
Azimuth: 110.00 to 140.00 step: 1.00 Elevation: 16.00 shots: 3
Missoula Fire Experiment
09NOV117.2D, 11/9/2001, 16:44, 260488
Azimuth: 110.00 to 140.00 step: 1.00 Elevation: 16.00 shots: 3
Missoula Fire Experiment
09NOV118.2D, 11/9/2001, 16:44, 260488
Azimuth: 110.00 to 140.00 step: 1.00 Elevation: 16.00 shots: 3
Missoula Fire Experiment
09NOV119.2D, 11/9/2001, 16:45, 260488
Azimuth: 110.00 to 140.00 step: 1.00 Elevation: 16.00 shots: 3
Missoula Fire Experiment
09NOV120.2D, 11/9/2001, 16:45, 260488
Azimuth: 110.00 to 140.00 step: 1.00 Elevation: 16.00 shots: 3
Missoula Fire Experiment
09NOV121.2D, 11/9/2001, 16:45, 260488
Azimuth: 110.00 to 140.00 step: 1.00 Elevation: 16.00 shots: 3
Missoula Fire Experiment
09NOV122.2D, 11/9/2001, 16:46, 260488
Azimuth: 110.00 to 140.00 step: 1.00 Elevation: 16.00 shots: 3
Missoula Fire Experiment
09NOV123.2D, 11/9/2001, 16:46, 260488
Azimuth: 110.00 to 140.00 step: 1.00 Elevation: 16.00 shots: 3
Missoula Fire Experiment
09NOV124.2D, 11/9/2001, 16:46, 260488

Azimuth: 110.00 to 140.00 step: 1.00 Elevation: 16.00 shots: 3
Missoula Fire Experiment
09NOV125.2D, 11/9/2001, 16:47, 260488
Azimuth: 110.00 to 140.00 step: 1.00 Elevation: 16.00 shots: 3
Missoula Fire Experiment
09NOV126.2D, 11/9/2001, 16:47, 260488
Azimuth: 110.00 to 140.00 step: 1.00 Elevation: 16.00 shots: 3
Missoula Fire Experiment
09NOV127.2D, 11/9/2001, 16:47, 260488
Azimuth: 110.00 to 140.00 step: 1.00 Elevation: 16.00 shots: 3
Missoula Fire Experiment
09NOV128.2D, 11/9/2001, 16:48, 260488
Azimuth: 110.00 to 140.00 step: 1.00 Elevation: 16.00 shots: 3
Missoula Fire Experiment
09NOV129.2D, 11/9/2001, 16:48, 260488
Azimuth: 110.00 to 140.00 step: 1.00 Elevation: 16.00 shots: 3
Missoula Fire Experiment
09NOV130.2D, 11/9/2001, 16:48, 260488
Azimuth: 110.00 to 140.00 step: 1.00 Elevation: 16.00 shots: 3
Missoula Fire Experiment
09NOV131.2D, 11/9/2001, 16:48, 260488
Azimuth: 110.00 to 140.00 step: 1.00 Elevation: 16.00 shots: 3
Missoula Fire Experiment
09NOV132.2D, 11/9/2001, 16:49, 260488
Azimuth: 110.00 to 140.00 step: 1.00 Elevation: 16.00 shots: 3
Missoula Fire Experiment
09NOV133.2D, 11/9/2001, 16:49, 260488
Azimuth: 110.00 to 140.00 step: 1.00 Elevation: 16.00 shots: 3
Missoula Fire Experiment
09NOV134.2D, 11/9/2001, 16:49, 260488
Azimuth: 110.00 to 140.00 step: 1.00 Elevation: 16.00 shots: 3
Missoula Fire Experiment
09NOV135.2D, 11/9/2001, 16:50, 260488
Azimuth: 110.00 to 140.00 step: 1.00 Elevation: 16.00 shots: 3
Missoula Fire Experiment
09NOV136.2D, 11/9/2001, 16:50, 260488
Azimuth: 110.00 to 140.00 step: 1.00 Elevation: 16.00 shots: 3
Missoula Fire Experiment

Susan Major/RMRS/USDAFS
06/08/2004 03:08 PM

To Vladimir A Kovalev/RMRS/USDAFS
cc pbertram@fs.fed.us, rsusott@fs.fed.us
bcc
Subject Re: Agreement 01-JV-11222049-254

Thank you so much. This is all we needed.

Sue

Sue Major
Clerk, Grants & Agreements
970-498-1395
smajor/rmrs
smajor@fs.fed.us
Vladimir A Kovalev/RMRS/USDAFS

Vladimir A
Kovalev/RMRS/USDAFS
06/07/2004 02:07 PM

To Susan Major/RMRS/USDAFS@FSNOTES
cc rsusott@fs.fed.us, pbertram@fs.fed.us
Subject Re: Agreement 01-JV-11222049-254

This document is in the Attachment.

Penny: is this enough or we should also mail two copies?

Vladimir A. Kovalev
Missoula Fire Sciences Laboratory
P.O.Box 8089, Missoula, MT 59807
Phone: 406-329-4862
FAX: 406-329-4863
Email: vkovalev@fs.fed.us

ForestServiceReport_Final.pdf

Ronald A Susott/RMRS/USDAFS

Ronald A
Susott/RMRS/USDAFS
06/07/2004 01:16 PM

To Susan Major/RMRS/USDAFS@FSNOTES
cc Penny M Bertram/RMRS/USDAFS@FSNOTES, Susan Major/RMRS/USDAFS@FSNOTES, Vladimir A Kovalev/RMRS/USDAFS@FSNOTES
Subject Re: Agreement 01-JV-11222049-254

Susan,

This is the U of Iowa-Eichinger agreement that was closed out long ago. I am sure we sent you the copies of the final report, but we will copy what we have and send two more.

Penny/ Vladimir: can you get a copy of Eichinger's report from our files, and provide copies for Susan?

Ronald A. Susott
Research Chemist
Rocky Mountain Research Station
Fire Sciences Laboratory
P.O. Box 8089
Missoula, MT 59807
Tel. (406) 329-4829
E-Mail: rsusott@fs.fed.us

Susan Major/RMRS/USDAFS

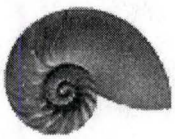

Susan Major/RMRS/USDAFS

06/07/2004 08:57 AM

To: Ronald A Susott/RMRS/USDAFS@FSNOTES, Penny M Bertram/RMRS/USDAFS@FSNOTES
cc: Susan Major/RMRS/USDAFS@FSNOTES
Subject: Agreement 01-JV-11222049-254

Agreement 01-JV-11222049-254 expired on 9/30/02, will you please send us two copies of the final report.

Thanks for your help.

Sue

Sue Major
Clerk, Grants & Agreements
970-498-1395
smajor/rmrs
smajor@fs.fed.us